



Single domain antibodies targeting pathological tau protein: Influence of four IgG subclasses on efficacy and toxicity

Erin E. Congdon,^a Ruimin Pan,^c Yixiang Jiang,^a Leslie A. Sandusky-Beltran,^a Andie Dodge,^a Yan Lin,^a Mengyu Liu,^d Min-Hao Kuo,^d Xiang-Peng Kong,^c and Einar M. Sigurdsson^{a,b*}

^aDepartment of Neuroscience and Physiology, and the Neuroscience Institute, New York University Grossman School of Medicine, 435 East 30th Street, New York, NY 10016, USA

^bDepartment of Psychiatry, New York University Grossman School of Medicine, New York, NY 10016, USA

^cDepartment of Biochemistry and Molecular Pharmacology, New York University Grossman School of Medicine, New York, NY 10016, USA

^dDepartment of Biochemistry and Molecular Biology, Michigan State University, 603 Wilson Road, Room 401, East Lansing, MI, 48824, USA

Summary

Background Eleven tau immunoglobulin G (IgG) antibodies have entered clinical trials to treat tauopathies, including Alzheimer's disease, but it is unclear which IgG subclass/subtype has the ideal efficacy and safety profile. Only two subtypes, with or without effector function, have been examined in the clinic and not for the same tau antibody. The few pre-clinical studies on this topic have only compared two subtypes of one antibody each and have yielded conflicting results.

Methods We selected two single domain antibodies (sdAbs) derived from a llama immunized with tau proteins and utilized them to generate an array of Fc-(sdAb)₂ subclasses containing identical tau binding domains but differing Fc region. Unmodified sdAbs and their IgG subclasses were tested for efficacy in primary cultures and in vivo microdialysis using JNPL3 tauopathy mice.

Findings Unmodified sdAbs were non-toxic, blocked tau toxicity and promoted tau clearance. However, the efficacy/safety profile of their Fc-(sdAb)₂ subclasses varied greatly within and between sdAbs. For one of them, all its subtypes were non-toxic, only those with effector function cleared tau, and were more effective in vivo than unmodified sdAb. For the other sdAb, all its subtypes were toxic in tauopathy cultures but not in wild-type cells, suggesting that bivalent binding of its tau epitope stabilizes a toxic conformation of tau, with major implications for tau pathogenesis. Likewise, its subclasses were less effective than the unmodified sdAb in clearing tau in vivo.

Interpretation These findings indicate that tau antibodies with effector function are safe and better at clearing pathological tau than effectorless antibodies. Furthermore, tau antibodies can provide a valuable insight into tau pathogenesis, and some may aggravate it.

Funding Funding for these studies was provided by the National Institute of Health (R01 AG032611, R01 NS077239, R01 NS120488, R21 AG 069475, R21 AG 058282, T32AG052909), and the NYU Alzheimer's Disease Center Pilot Grant Program (via P30 AG008051).

Copyright © 2022 The Authors. Published by Elsevier B.V. This is an open access article under the CC BY-NC-ND license (<http://creativecommons.org/licenses/by-nc-nd/4.0/>)

Keywords: Tau; Immunotherapy; Antibody subclass; Single domain antibody; Microdialysis; Primary culture; PHF

Abbreviations: AD, Alzheimer's disease; PSP, progressive supranuclear palsy; sdAb, single domain antibody; PBS, phosphate buffered saline; PBS-T, phosphate buffered saline with Tween 20; PHF, paired helical filament; IgG, immunoglobulin G; BLI, bio-layer interferometry; ELISA, enzyme linked immunosorbent assay; LDH, lactate dehydrogenase; BCA, bicinchoninic acid; ISF, interstitial fluid; aCSF, artificial cerebrospinal fluid; BSA, bovine serum albumin; CT, computed tomography; IACUC, Institutional animal care and use committee; PBMC, peripheral blood mononuclear cells; IL-2, interleukin-2

*Corresponding author at: Department of Neuroscience and Physiology, and the Neuroscience Institute, New York University Grossman School of Medicine, 435 East 30th Street, New York, NY 10016, USA.

E-mail address: enar.sigurdsson@nyulangone.org (E.M. Sigurdsson).

Research in context

Evidence before this study

About half of tau antibodies in clinical trials are on a human IgG4 backbone, whereas the other half employs a human IgG1 subclass. The former lacks effector function and is chosen to minimize inflammation, whereas the latter activates microglia and is selected to enhance efficacy. However, data on which tau antibody subclass has the best efficacy/safety profile is very limited and contradictory. There are no prior reports comparing the efficacy/safety profile of all tau antibody subclasses. Such comparison is of major importance to the field of tau immunotherapies.

Added value of this study

We have generated novel single domain antibodies against the tau protein, and derived from them IgG1, IgG2A, IgG2B, and IgG3 murine antibody subclasses with identical tau binding regions. This allowed us to thoroughly examine the impact of subclass on antibody safety and efficacy in targeting both extra- and intracellular tau. Our data show that antibodies with effector function are safe, can work inside and outside cells, and are more efficacious than antibodies lacking effector function. Additionally, one of the single domain antibodies became toxic when rendered bivalent, indicating that it stabilized a pathological tau conformation, and thereby provided a valuable insight into tau pathogenesis.

Implications of all the available evidence

Tau antibodies with effector function are safe and more efficacious than effectorless antibodies. Efficacious univalent antibodies can become toxic when made bivalent, which should be taken into account during antibody engineering designed to improve their efficacy/safety profile.

Introduction

In the last 15 years, tau immunotherapies have advanced from proof-of-concept studies to over a dozen clinical trials (for recent reviews see^{1–6}). Some of those trials have failed and there are some likely reasons for that. Specifically, most of the failed antibodies target the N-terminus of tau and were originally described to only work extracellularly. Firstly, the amount of the tau protein outside cells is only a small fraction of its total pool, with most of it being found within cells, particularly in neurons.^{7,8} Secondly, most of extracellular tau consists of its mid-domain, roughly amino acids 150–250, with the N- and C-terminus having been degraded following its release from the cell.^{9–11} Thirdly, the tau protein is not increased in cerebrospinal fluid in primary tauopathies, such as progressive supranuclear palsy (PSP), compared

to age-matched controls,^{9,12–17} indicating that extracellular tau is likely not increased in those diseases. Considering these points, it is not particularly surprising that many of the N-terminal antibodies have been discontinued in primary tauopathies and in AD patients.

It is too early to tell which antibody subclass will have the best efficacy/safety profile. At this point, only human IgG1 and IgG4 of IgG subclasses are in clinical trials. The former, IgG1, has a strong effector function, including promoting phagocytosis of antibody-tau complex. This should enhance its efficacy, in particular if it only works extracellularly, but phagocytosis may be associated with inflammation. The latter, IgG4, has a limited effector function, which may curtail its extracellular efficacy if microglial phagocytosis is important for tau clearance, but reduces potential inflammatory side effects. The other human IgG subclasses, IgG2 and IgG3 have not been examined in clinical tau antibody trials. While evidence is limited, the general concern over inflammation has presumably led to IgG4 being selected in around half of the clinical trials. It has been argued that effector function is not necessary for efficacy, and potentially harmful,¹⁸ whereas others report that human IgG1 with tau in cultured microglia does not increase cytokine release over tau alone.¹⁹ Indeed, our group and many others have utilized tau antibodies with effector function in vivo without adverse immune responses. Whether activation would indeed be harmful is also potentially in question as the mRNA expression pattern seen when glia were activated with tau antibodies is not the same as with bacterial lipopolysaccharides.²⁰ Adding to the complexity of the issue is the debate surrounding microglia in the context of tau pathology. Ablation of microglia has been found to be protective, detrimental, or neutral with respect to tau pathology and neurodegeneration in different reports, and activation has been linked to spreading of tau aggregates.^{21–28} Others have seen no difference in glial tau processing following exposure to inflammagens.²⁹ However, activation induced by uptake of tau alone vs tau-antibody complex may not be the same.

Prior work on tau antibody subclasses in tauopathy models has been limited. Two groups have compared the efficacy of human IgG1 and IgG4 subclasses. Genentech reported that both subclasses of the tau antibody Semorinemab showed similar efficacy in preventing tau oligomer induced toxicity in isolated neuronal cultures.³⁰ However, in mixed neuron/glia cultures only the IgG4 variant was protective, whereas the IgG1 subclass was effective at a lower dose in vivo. Axon Neuroscience generated IgG1 and IgG4 variants of AX004, a humanized version of truncated tau antibody DC8E8, and showed that the IgG1 was more effective than the IgG4 in promoting tau uptake in primary human microglial cultures.¹⁹ For both subclasses of DC8E8, the Fc portion of the antibody was required for phagocytosis. Further, blocking FcγII/III receptors also reduced

microglial uptake. In a third study, Bajracharya et al. examined the efficacy of the tau antibody RN2N in isolated mouse microglia and in a mouse tauopathy model.³¹ As expected, the mouse IgG2A (full effector function, comparable to human IgG1) promoted glial phagocytosis of tau more effectively in culture than the mouse IgG1 (less effector function). However, the two subclasses had a similar effect in the mice on clearing several soluble and insoluble phospho-tau epitopes as quantified on western blots, although the IgG1 subclass appeared to be more effective in clearing a particular phospho-tau epitope on immunostained brain sections. Overall, the outcome of these prior studies is rather contradictory, indicating that this important issue needs to be further examined.

With this in mind, we set out to systematically examine the efficacy and safety profile of tau antibodies, consisting of all of the mouse IgG subclasses. Initially, we focused on single domain antibodies (sdAbs), derived from llamas, which because of their unique properties, have a great therapeutic potential, including as gene therapies. We then selected two of those to be engineered as Fc(sdAb)₂ into different mouse Fc subclasses. Importantly, two of the subclasses, were most and equally effective, mouse IgG1 and IgG2A, which are close to human IgG2 and IgG1, respectively. Mouse IgG3, which is comparable to human IgG4, was the least effective subclass. Interestingly, one of the sdAbs, which was effective in clearing pathological tau and preventing its toxicity became toxic and rather ineffective in all of its subclass Fc(sdAb)₂ forms, suggesting that its bivalency stabilized a toxic conformation of the tau protein.

Overall, these findings have important implications for therapeutic development of tau antibodies and for understanding tau pathogenesis.

Methods

Generation of antibodies

Single domain antibodies (sdAbs) were generated by using the services of ProSci Inc (Poway, CA). An adult llama was immunized 7 times over the course of 188 days. The first 5 immunizations were with full length recombinant 2N4R human tau (rec-tau) and the last 2 vaccinations were with paired helical filament enriched pathological tau isolated from a human patient displaying mixed Alzheimer's disease (AD) and Pick's disease pathology (National Disease Research Interchange, Philadelphia, PA) as described previously.^{32,33} The first immunization (subcutaneous (s.c.), 200 µg rec-tau) was in complete Freund's adjuvant (CFA; Sigma), the second one in incomplete FA (IFA (Sigma), s.c., 100 µg rec-tau), the third to fifth in IFA (s.c., 100 µg rec-tau) and Adjuvax (Sigma, s.c. 100 µg rec-tau), and the sixth and seventh in Adjuvax (200 µg PHF)

split between s.c. and intramuscular (i.m.). Blood was collected from the animals every 28 days, and RNA was isolated from peripheral blood mononuclear cells (PBMC) obtained from bleeds 4 and 6 together. Random hexanucleotide primers and SuperScript reverse transcriptase were used to synthesize cDNA from the samples. This cDNA was used to clone the sdAbs using a two-step PCR process. In the first reaction, all heavy chains from sdAbs and whole antibodies were amplified using CaL1/CaL2 primers: 5'-GTCTGGCTGCTCTTCTACAAGG-3' / 5'-GGTACGTGCTGTTGAACTGTTCC-3'. sdAbs were then specifically amplified using primers proprietary to ProSci. The products of this second reaction were gel purified and cloned into the pADL-23c vector and used to transform *E. coli* TG1 cells.

Solid and solution phase panning was carried out using polystyrene beads coated with 2N4R rec-tau. The bacterial supernatants of numerous clones were evaluated for binding to various tau preparations from different sources (rec-tau, and tau fractions from human and mouse tauopathy brains). Six clones, representing different binding profiles within the cohort, were initially selected, endotoxin purified and their efficacy in culture models evaluated. Two of the most efficacious ones were then chosen for further evaluation. These clones were then transfected into mammalian cells for purification and used to generate whole mouse IgG1, IgG2A, IgG2B and IgG3 antibodies.

For the unmodified 2B8 and 1D9 sdAbs, the pVRC8400-sdAb constructs were made by inserting their individual gene sequences between the 5' EcoRI and 3' AfeI sites with signal peptide, mouse interleukin-2 (IL-2) leader sequence (MYRMQLLSICIALSLALVT), at N-terminus and myc-his tags at C-terminus for detection and purification. The sdAbs were then expressed in FreestyleTM 293F cells (Invitrogen, Cat. No. R790-07). Briefly, FreestyleTM 293F cells were transiently transfected with the mixture of DNA plasmid and polycation polyethylenimine (PEI; 25 kDa linear PEI, Polysciences, Inc., cat. No. 23966). The transfected cells were incubated at 125 rpm in FreestyleTM 293 Expression Medium for suspension culture at 37°C with 5% CO₂. The supernatants were harvested 5 days after transfection, filtered through a 0.45 µm filter, followed by sdAb purification using Ni-NTA columns (GE Healthcare).

Likewise, pVRC8400 plasmids containing each of the mouse IgG subclasses were utilized to produce the sdAb subclasses. The 1D9 and 2B8 variable regions were inserted between the 5' EcoRI and 3' AfeI sites of the pVRC8400 plasmid using the mouse interleukin-2 (IL-2) leader sequence (MYRMQLLSICIALSLALVT). The existing C_{H1} regions were deleted, and a hinge region added to link the sdAbs to the C_{H2} and C_{H3} constant domains (hinge sequences: PRDCGCKPCICT, PRGPTIKPCPPCKCP, PSGPISTINPCPPCKECKKCP, and PRIPKPSTPPGSSCP, for IgG1, IgG2A, IgG2B, and

IgG3 respectively). Plasmids containing each subclass were used to transiently transfect Freestyle™ 293F cells in suspension cultures. Transfected cells were maintained in serum free FreeStyle™ 293F media at 37°C with 5% CO₂. Culture supernatant was harvested 5 days post transfection, filtered, and then purified using immobilized Protein A or Protein G columns. Antibodies were eluted using IgG elution buffer (0.1 M glycine, pH 2.7) and neutralized immediately with 1 M Tris buffer (pH 8.5). Protein concentration was determined using a BCA assay.

Isolation of paired helical filament tau

Paired helical filament (PHF)-enriched tau was isolated from human tissue obtained from patients with mixed AD/Pick's disease pathology and mixed AD/Progressive supranuclear palsy (PSP) (National Disease Research Interchange, Philadelphia, PA) using methods described previously.^{32,33} These samples were chosen for their ability to induce robust toxicity in preliminary experiments using primary neuronal and mixed neuron/glia cultures. Brain tissue was homogenized in buffer containing 0.75 M NaCl, 1 mM EGTA, 0.5 mM MgSO₄, and 100 mM 2-(N-morpholino) ethanesulfonic acid (pH 6.5) and centrifuged at 11,000 x g for 20 min. The resulting low speed supernatant was then incubated with 1% sarkosyl (from 10% solution dissolved in PBS) for one hour at room temperature. This mixture was centrifuged at 100,000 x g for 60 min. The supernatant was removed, and the pellet washed with the 1% sarkosyl solution. The tau was then resolubilized by being briefly heated to 37°C in 50 mM Tris-HCl buffer, and then dialyzed in PBS overnight.

Preparation of recombinant hyperphosphorylated tau

Recombinant hyperphosphorylated tau (p-tau) was purified as previously described.³⁴ Briefly, the 1N4R isoform of tau was expressed along with GSK-3β via the PIMAX approach.³⁵ The BL21 Codon plus strain bearing the p-tau expressing plasmid was grown at 37°C until OD₆₀₀ reached between 0.3 and 0.5 before two h induction with 0.5 mM of IPTG. Cell pellets were suspended in purification buffer (20 mM Tris-HCl pH 5.8, 100 mM NaCl, 1 mM PMSF, 0.2 mM orthovanadate) and treated with 1 mg/ml lysozyme at 30°C for 30 min. The mixture was then sonicated (Branson Digital Sonifier 450; 30% amplitude; total process time 3 min; pulse-ON time 5 sec; pulse-OFF time 5 sec) and centrifuged at 17,000 x g for 40 min at 4°C. The supernatant was left in a boiling water bath for 30 min and left on ice for 30 min with occasional gentle shaking. After centrifugation at 17,000 x g for 50 min at 4°C, the supernatant was transferred to another tube and supplied with a final concentration of 0.5 mM DTT and 1 mM EDTA. One OD₂₈₀ of purified recombinant TEV protease was added to digest each 100 OD₂₈₀ of the sample overnight at 4°C. The

digestion mixture was then centrifuged at 17,000 x g for 30 min at 4°C. The supernatant with p-tau was collected and concentrated by centrifugation through a spin column (Amicon Centrifugal Filter Unit, Ultra-15, 10K). A gel filtration buffer (20 mM Tris-HCl pH 7.4, 100 mM NaCl) was added at the end of the concentration step. The centrifugation and buffer change were repeated twice. The final gel filtration buffer equilibrated solution was injected to a Superdex 200 10/300 GL column (GE Healthcare Life Sciences, USA). Size exclusion chromatography was done on an AKTA explorer FPLC unit at 4°C under a flow rate of 0.3 ml/min. Fractions containing p-tau were pooled and concentrated by a spin column. After the concentration was completed, the protein solution was collected and supplemented with 10% glycerol (v/v) before -80°C storage.

Bio-layer interferometry affinity assay

In the biolayer interferometry (BLI) affinity assay, recombinant (rec) tau used in the solid phase binding experiments was first biotinylated using EZ-Link™ NHS-PEG4-Biotin. Tau was incubated with the biotin reagent for 30 min at room temperature, and then dialyzed. Prior to testing, the streptavidin (SA) biosensors were hydrated in phosphate buffered saline containing 0.01% Tween-20 (PBS-T) for 10 min. Initial baseline measurements were performed for 120 sec, after which 400 nM of the biotin labeled tau was added for a further 120 sec to load the probe. After this step, an additional baseline reading was collected. Association was conducted for 300 sec using increasing concentrations of sdAbs or their subclasses, and dissociation for 400 sec. Readings were also collected from a reference biosensor loaded with biotinylated tau and incubated with buffer alone during the association and dissociation steps. Sensor tips were regenerated by alternating incubation with 10 mM glycine (pH 2.0) and assay PBS-T.

For solution phase experiments where the tau antibodies were immobilized, two types of sensors were used. For the sdAbs, Ni-NTA sensors pre-immobilized with nickel-charged tris-nitrilotriacetic (Tris-NTA) were utilized to capture the histidine tagged single domain antibodies. Baseline readings were obtained in PBS-T for 120 sec, after which the probes were loaded by incubating the probes with 5 μg/ml of the sdAbs for 120 sec. After antibody binding, sdAb loaded biosensors were dipped into solutions containing either rec-tau, p-tau, or solubilized human-derived PHF-tau. In these experiments 1-3% NTA agarose was added to the standard PBS-T assay buffer to reduce non-specific binding. As above, association was measured for 300 sec, and dissociation for 400 sec. The probes were regenerated using 10 mM glycine and PBS-T, and then recharged with 10 mM NiCl₂.

For the whole antibody subclasses, anti-mouse IgG Fc Capture (AMC) probes were utilized. Sensors were hydrated, and then alternately incubated with 10 mM

glycine and PBS-T for 20 sec each to improve baseline and surface stability. Whole antibodies were then added at 5 $\mu\text{g}/\text{ml}$ for 120 sec to load the probes. After loading, the experiments were conducted as described above, with an additional baseline, 300 sec for association, and 400 sec for dissociation in solutions containing rec-tau, p-tau, and PHF-tau. As in the other tests, a loaded probe was also included that was incubated in PBS-T with no tau present. Sensors were refreshed by alternating incubation with 10 mM glycine and PBS-T. It should be noted that the IgG3 subtype did not bind to the AMC probe so its affinity for the different tau targets could not be examined.

All BLI binding experiments were conducted at room temperature in black 96 well plates, using a ForteBio Octet[®] RED96. Data was analyzed using Data Analysis 11.0 software. The measurements from probes exposed to blanks were subtracted and a 1:1 binding model was used. To allow curve fitting for both association and dissociation steps, negative responses were inverted using the “flip” function. Data were analyzed globally by fitting the curves for multiple concentrations at the same time using a 1:1 binding model with the same rate constants. Using this method provides a more robust and accurate estimate of the binding constants.

Animals

All animals were housed in Institutional Animal Care and Use Committee (IACUC) approved facilities, with access to food and water ad libitum, and experiments were performed under an IACUC approved protocol. Animals undergoing microdialysis had ad libitum access to food and water during the procedure, and were able to move freely in the RaTurn apparatus. The JNPL3 tauopathy mouse line (RRID:IMSR_TAC:2508) was used for both in vivo microdialysis experiments and to generate mixed neuron/glia and neuronal cultures. For whole animal studies, females aged 7–11 months were utilized. Animals were given post operative care and euthanized using methods consistent with guidelines provided by the Panel on Euthanasia of the American Veterinary Medical Association (for additional details see the in vivo microdialysis section). Cell cultures were made from pups collected at postnatal day 0. The JNPL3 mouse line expresses the human oN4R tau isoform containing the naturally occurring P301L mutation found in human frontotemporal dementia, in addition to the native mouse tau.³⁶ Pups from wild-type mice of the same genetic strain background were used at postnatal day 0 to generate the wild-type cortical cultures. Pups were removed from the home cage and euthanized via decapitation.

Preparation of mixed cortical and primary neuronal cultures

Cultures were prepared from JNPL3 pups at postnatal day 0 as previously described. Briefly, plates were coated

with Pluripro (Cell Guidance Systems) for at least 3 h. The cortex and hippocampus of each mouse was removed and washed in modified Hank's Balanced Salt Solution. Tissue was incubated with 0.5% trypsin for 20 min at 37°C, and then subjected to further washing and manual dissociation. Cells to be used for the mixed cortical cultures were maintained in plating media containing glucose and serum. To remove the glia and produce neuronal cultures, the plating media was removed after the first 24 h and replaced with neurobasal media.

Cell culture efficacy experiments

The efficacy of each unmodified univalent sdAb in clearing pathological tau or preventing tau-induced toxicity and seeding was tested in primary neuronal cultures. In the first set of experiments, JNPL3 cells were incubated with 10 $\mu\text{g}/\text{ml}$ of each sdAb for seven days to determine whether they could induce the clearance of natively expressed tau, and to test for any toxic effects of the antibodies themselves. In the second set, we utilized the sdAbs in combination with human-derived PHF-tau in two different dosing paradigms that mimic extra- and intracellular mechanisms. To simulate extracellular blockage of tau spreading, we added the PHF and sdAbs to the culture at the same time (PHF + Ab) and allowed them to incubate together in the media for 24 h. After this time, the media was replaced, and the cells were maintained in culture for a further seven days. Intracellular clearance was modelled by adding the PHF to the neuronal cultures first and allowing the cells to take up the pathological protein for 24 h. Media was then exchanged, and the antibody was added (PHF \rightarrow Ab). Because the PHF is already internalized in this paradigm, the antibody must also enter the cells to be effective. Efficacy experiments were carried out in JNPL3 mixed neuron/glia cultures using the same dosing paradigms (PHF + Ab and PHF \rightarrow Ab). Samples were collected 96 h following antibody application.

The use of a 7 day incubation, 1 $\mu\text{g}/\text{ml}$ PHF and 1 $\mu\text{g}/\text{ml}$ antibody in the neuronal cultures was chosen based on previously published results.^{32,33} The selection of a 96 h incubation time and 10 $\mu\text{g}/\text{ml}$ PHF in the mixed cultures was determined in preliminary testing using PHF alone. A higher dose is required to achieve toxicity, presumably due to the trophic support provided by the glial cells and their neutralization of PHF. In these preliminary tests, we observed robust pathological changes after 4 days.

For all experiments, a set of Day 0 untreated controls were collected from the same plate prior to treatment. An addition group of cells was also left untreated and collected together with the experimental groups once the incubation was complete, either on Day 7 or at 96 h. When analyzed, all groups were compared to their respective Day 0 untreated controls. By including two untreated groups, we ensure that changes seen in the

tests are not the result of spending an additional 4–7 days in culture. Furthermore, all samples in the same plate were prepared from the same animal to control for any variation in protein expression between mice, and the overall age of the culture.

Lactate dehydrogenase assay

The lactate dehydrogenase (LDH) assay kit was used per manufacturer's instructions (Roche, Mannheim Germany). Briefly, media from each sample was added to a 96 well plate and incubated with colourimetric agent at room temperature for 30 min. Data was collected using a Bio Tek Synergy 2 plate reader. Data was normalized using the total protein concentration per sample as determined using a Bicinchoninic acid (BCA) assay.

Immunoblotting

Immunoblotting was conducted as previously described.^{32,33} Cultured neurons were washed in PBS and then lysed in 250 μ l of RIPA buffer (50 mM Tris-HCl, 150 mM NaCl, 1 mM EDTA, 1% Nonidet P-40, 1X protease inhibitor cocktail (cOmplete, Roche), 1 mM NaF, 1 mM Na₃VO₄, 1 mM PMSF, 0.25% sodium deoxycholate, pH 7.4). All samples were assayed for total protein concentration using a BCA assay and levels normalized. On each gel, untreated control samples prepared from the same animal were run along with those of the experimental conditions to serve as an internal control. All samples were then added to O+ loading buffer (62.5 mM Tris-HCl, 10% glycerol, 5% β -mercaptoethanol, 2.3% SDS, 1 mM EDTA, 1 mM EGTA, 1 mM NaF, 1 mM Na₃VO₄, 1 mM PMSF, 1X protease inhibitor cocktail (cOmplete, Roche), and boiled for 5 min. The same amount of total protein was added to each well. Cell lysate was run on a 12% polyacrylamide gel and then transferred to nitrocellulose membranes. Blots were probed with antibodies against neuronal marker NeuN (RRID:AB_10807945), total tau (RRID:AB_10013724) and tau phosphorylated at Ser199 (RRID:AB_2533737) at 1:1000 dilution in SuperBlock (Invitrogen) overnight at 4°C. Each experiment was carried out using cells prepared from the same animal to limit variability. Membranes were incubated in HRP-conjugated rabbit secondary antibody (1:5000, RRID:AB_228341) for one h at room temperature. In all experiments, chemiluminescent signal was visualized using a Fuji LAS-4000 and quantified with Image J (RRID:SCR_003070). NeuN was selected as a marker of cytotoxicity,^{32,33,37–42} as its levels reflect retraction of neuronal processes, a decrease in cell volume, and metabolic toxicity as well as overt cell loss. GAPDH levels are altered with PHF to a similar degree as NeuN in our cultures. Cytoskeletal proteins commonly used as controls may also be altered when cultures are exposed to pathological tau.^{43–50}

As stated above, all blots contain a set of untreated cells collected at Day 0. Changes in NeuN and tau levels were first determined for each blot individually by calculating the change in chemiluminescent signal relative to their internal Day 0 controls. NeuN exists as two splice variants that can be visualized as one or two bands with apparent molecular weights between 40 and 50 kD,⁵¹ depending on buffer conditions, the percentage of acrylamide in the gels, electrophoresis time, and binding to the primary antibody. In rare cases, two bands may be visible in some samples but not in others from the same pool of cells (see Figure 7c). In all experiments, whenever two bands were visible in the blots, both were quantified. Once the percent change in NeuN, or tau/NeuN ratios were determined for each individual blot, the data from replicate experiments were then combined.

CypHer 5 labeling

Each of the 1D9 and 2B8 subclasses were labeled using CypHer 5, which fluoresces only in low pH conditions such as inside endo- and lysosomes. This feature allowed us to confirm that any signal detected was truly intracellular. Antibodies were incubated with the dye for one h at room temperature in a solution of PBS and carbonate buffer (pH 8.3). Following this, the antibodies were dialyzed in PBS overnight to remove any unbound dye. Protein concentration and labelling efficiency were then determined.

Microscopy and quantitation

Cultures used for imaging were prepared as described above on glass bottom plates. Images were collected using an Axio Observer inverted confocal microscope at 20x magnification. To quantify the extent and cell type of uptake, in antibody alone and antibody + PHF conditions, we utilized both live cultures and fixed cells on coverslips.

We first examined the extent of antibody uptake and colocalization with neurons. For this experiment, live cultures were incubated with 5 μ g/ml CypHer 5 labeled antibodies alone for one h. An additional group of cells grown on glass coverslips was fixed and stained using total tau antibody to visualize neurons. Images were collected and used to determine the overall cellular uptake and colocalization with neurons. We also determined the extent and cell type of uptake for each 1D9 subclass in the presence of exogenous PHF. All cultures were incubated with 5 μ g/ml of the CypHer 5 labeled 1D9 antibodies, 1 μ g/ml PHF, and tomato lectin to visualize microglia for one h before imaging.

To quantify antibody uptake the images were imported into Image J. Threshold was adjusted, and the percentage of pixels containing the antibody signal was determined. To determine the percentage of neuronal and microglial uptake we used a colocalization macro in

Image J which determined the overlap of the two fluorescent signals.

Enzyme linked immunosorbent assays

We performed two types of enzyme linked immunosorbent assays (ELISAs) to determine the binding of each subclass to PHF-tau. In the first, plates were coated with solubilized PHF, sarkosyl insoluble, or sarkosyl soluble tau fractions from a human tauopathy brain with mixed AD/Pick's disease pathology at 1 µg per well overnight at 4°C. Following coating, plates were washed and blocked for 30 min at room temperature in Superblock. Antibodies were brought to the same starting concentration and serial dilutions of each subclass were added to the plate. Plates were incubated for a further two h at room temperature, washed with TBS-T, and then mouse secondary (1:5000) was added for one h. Plates were then washed and developed as above.

A single antibody concentration was chosen for the competitive ELISA, and the subclasses were incubated with increasing concentrations of PHF (0 – 200 ng) for 30 min before being added to the plate. Following this preincubation, the procedure was identical to the standard ELISA using plates coated with solubilized PHF.

Additional ELISAs were carried out to determine the concentration of tau in interstitial fluid samples collected by microdialysis using a commercially available kit (ThermoFisher Cat# KHB0041).

In vivo microdialysis

In vivo microdialysis was performed as previously described,⁵² with minor modifications. On the day of sampling, and prior to the start of surgery, peptide microdialysis probes (1,000,000 Da MWCO; AtmosLM, Amuza Inc.), santopren tubing (SciPro), and FEP tubing (Zeus Inc) were flushed with Proclin (Sigma) and then filled with standard perfusate (artificial cerebrospinal fluid; aCSF⁵³ containing 0.15% bovine serum albumin (BSA) (Sigma) and allowed to equilibrate for one h prior to sample collection. All samples were collected under constant light.

After probe calibration, female JNPL3 mice aged 7–11 months were anaesthetized with isoflurane (3% for induction, 1.5–2.0% for maintenance) and placed in a stereotaxic frame with a heating pad to maintain normal body temperature. A single hole was drilled at coordinates 3.0 mm post bregma, +2.5 mm lateral of the midline, and 1.2 mm ventral from dura at a 12° angle, allowing a microdialysis guide cannula and a dummy probe to be inserted into the left hippocampus. Correct probe placement was confirmed initially by a computed tomography (CT) scan (Supplemental Figure 1). Guide cannulas were affixed to the skull using bone screws and dental cement. All animals were monitored following surgery and given twice daily injections of buprenorphine (0.05–1 mg/kg). Thirty to sixty min after the completion of surgery, the dummy probe was replaced

with a 2 mm microdialysis probe and animals were placed in a RaTurn microdialysis cage (Bioanalytical Systems Inc.; BASi) for the remainder of sampling. Importantly, the RaTurn housing apparatus allows for unrestricted movement at all-times, which allows for endogenous behaviors such as running, grooming, nesting and sleeping throughout microdialysis sampling. The hippocampus of each animal was continuously perfused at a rate of 1.2 µl/min using a syringe pump (KD Scientific). Simultaneously, brain interstitial fluid (ISF) was collected using a peristaltic pump (MAB 20, SciPro) at a rate of 1.0 µl/min. ISF samples were collected in a refrigerated fraction collector (BASi) in one h intervals with the first 18 h treated as a recovery period. The next 8 h were used to establish a baseline for extracellular tau levels during the animals' inactive period. Following this, animals received via reverse dialysis 50 µg/mL of 1D9 or 2B8 sAb (total of 7.2 µg injected), or the equivalent molar concentration of their IgG1 and IgG2A subtypes in a two h infusion taking into account their two binding sites. Treatment groups were assigned randomly. In each session, sampling was performed on 2–3 animals at the same time with a mix of control and treatment groups represented. After the two h infusion period, animals were switched back to standard perfusate and samples were then collected for an additional 22 h. Untreated control animals were given identical surgeries with samples collected in an identical manner but receiving only aCSF. No animals died before the completion of the testing. Following the experiment, animals were anesthetized with an overdose of ketamine/xylazine prior to transcardial perfusion and decapitation. This method is consistent with the recommendations of the Panel on Euthanasia of the American Veterinary Medical Association. After collection, samples were pooled into fractions representing two h increments and assayed for total tau levels using the ELISA kit referenced above. For analysis, percent baseline for each mouse was calculated by averaging each animal's own baseline samples (samples preceding treatment infusion) and then dividing all of the animal's samples by this average baseline. In this way we determined the relative percent change from each animal's own baseline and corrected for any basal differences in ISF tau between mice and across groups.

Statistics

Data was analyzed using GraphPad version 9.3 (RRID: SCR_002798). For the cell culture efficacy and uptake data a standard one-way ANOVA was utilized, with Tukey's multiple comparisons test, except for the sAb uptake experiments where there were two data sets, a standard t test was utilized. For the ELISA, wild-type culture time course, and in vivo time course data, a two-way ANOVA was used to determine significant differences between the antibodies at different concentrations or times, with Tukey's multiple comparisons test for

differences between individual points. A standard one-way ANOVA was used on the pooled post-treatment microdialysis samples with Tukey's multiple comparisons.

In all experiments we aimed to ensure an adequate sample size and robustness in the data. All culture treatment groups contained at least six replicates per group, and each plate included internal controls. Sample numbers were based on previous experience using cultured cells. The choice of image analysis was made with the goal of reducing potential bias. Each investigator was aware of the group allocations and conditions in their experiments. No data from either culture or in vivo experiments was excluded from the final analysis.

Ethics

All the procedures involving animals were approved by the IACUC committee of the university, and are in accordance with NIH Guidelines, which meet or exceed the ARRIVE guidelines. All animals housed at NYU Grossman School of Medicine animal facilities are cared for by the Division of Laboratory Animal Resources (DLAR) veterinary staff in a AAALAC approved facilities. All animal studies were carried out using protocols approved by IACUC. The DLAR director is board certified by the American College of Laboratory Animal Medicine (ALAM) and is licensed to practice veterinary medicine in the State of New York. All members of the lab working with animals have received training in ethics and animal handling from the New York University Grossman School of Medicine (Animal Welfare Assurance number D16-00274).

Role of funders

Funding agencies were not involved in the design or implementation of the experiments and did not contribute to data analysis or the writing of this report.

Results

Single domain antibodies bind to recombinant-, phospho-, and paired helical filament-enriched-tau

Single domain antibodies (sdAbs) were generated by immunizing llamas with 2N4R recombinant (rec) tau and human derived paired helical filament (PHF) tau. Multiple clones were purified, and two candidates, 1D9 and 2B8, were selected for further testing. The polyclonal tau sdAb (poly sdAb), from which these monoclonals were derived was included in certain assays for reference.

Solution phase: Overall sdAb binding to rec-tau was 1 to 3-fold higher in solution phase than in solid phase, with 2B8 having higher affinity (14.2 nM) than 1D9 (39.7 nM) and poly sdAb (59.8 nM, Supplemental Table 1, Figure 1a-c).

The three sdAbs had very similar affinities for p-tau (32.6 – 33.4 nM, Supplemental Table 1 and Figure 1d-f), whereas their affinity differed for human derived PHF-tau (1D9: 25.0 nM; 2B8: 141.5 nM; poly sdAb: 43.4 nM, Table S1, Figure 1g-i).

Solid phase: The 1D9 and 2B8 sdAbs had similar affinities for rec-tau in solid phase ($K_D = 50.8$ nM and 49.3 nM), with the poly sdAb having about 2-fold lower binding (108.1 nM, Supplemental Table 1, Figure 1j-l).

1D9, 2B8, and polyclonal sdAbs are not toxic to neurons

Primary neuronal cultures prepared from JNPL3 tauopathy mice were incubated with 1 µg/ml of 1D9, 2B8, and poly sdAbs for 7 days, followed by collection of media and cell lysate to determine if the sdAbs alone induced toxicity in the cells.

Lactate Dehydrogenase (LDH) levels: The sdAbs and the untreated controls did not differ in their culture media LDH levels (Supplemental Figure 2a).

NeuN levels: Likewise, these groups did not differ in their NeuN levels as examined by immunoblotting of cell lysates (Supplemental Figure 2b).

Collectively, these results indicate that the sdAbs alone are not toxic to neurons.

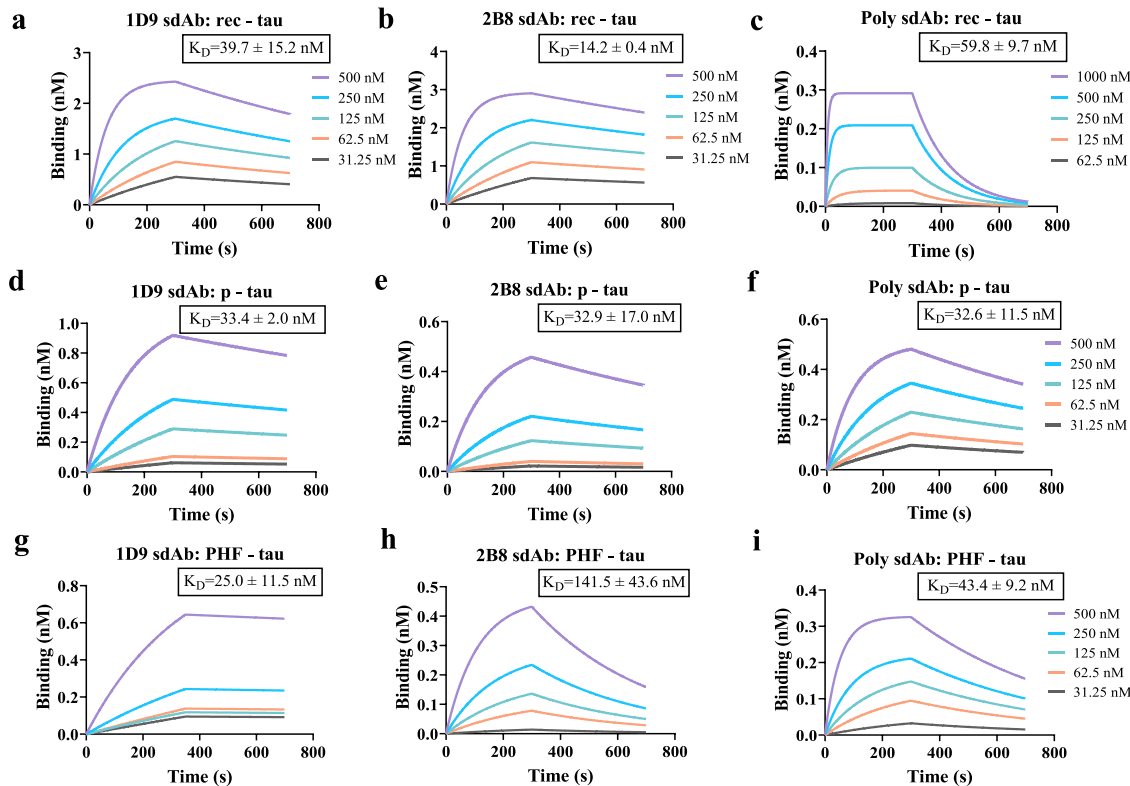
1D9 and 2B8 sdAbs are readily internalized by cultured neurons

To prepare for the treatment paradigms, primary neuronal cultures prepared from JNPL3 mice were incubated with 1 µg/ml CypHer 5 labelled sdAbs for 24 h. Cultures were then imaged live and the percentage of pixels containing fluorescent signal was determined. The CypHer 5 tag will only fluoresce when in an acidic environment, such as in the endosomal/lysosomal system within neurons. Both monoclonal sdAbs were readily taken up into neurons, with the signal concentrated in the soma (Supplemental Figure 3a). Their uptake was comparable with a similar percentage of positive signal per image (Supplemental Figure 3b).

1D9, 2B8, and poly sdAbs prevent PHF-induced toxicity and pathological seeding in neuronal cultures

Initial efficacy testing of the sdAbs was conducted in primary neuronal cultures prepared from JNPL3 mice. Cells were incubated with 1 µg/ml human derived PHF-enriched tau and either 1D9, 2B8, or poly sdAbs using the PHF + Ab and PHF → Ab dosing paradigms. As described in the Methods section, these different approaches were used to simulate extracellular (PHF + Ab), and intracellular (PHF → Ab) targeting of pathological tau. Culture media and cell lysate were probed for LDH and NeuN levels, respectively. Lysates from the same samples were also probed for total

Solution phase BLI binding assay- unmodified sdAbs



Solid phase BLI binding assay- unmodified sdAbs

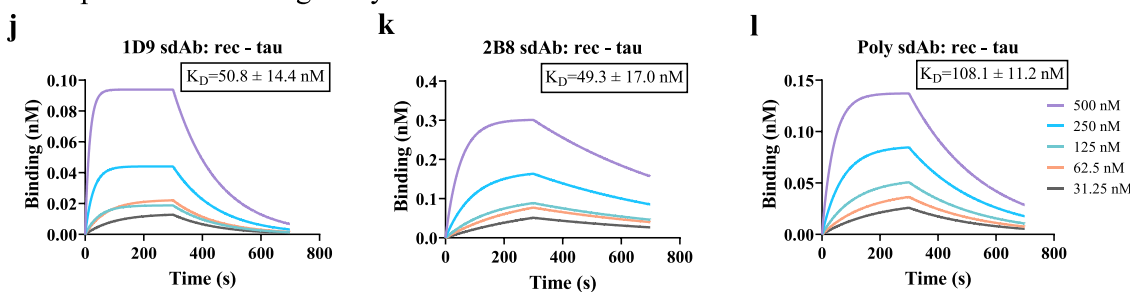


Figure 1. 1D9, 2B8, and tau polyclonal sdAbs bind recombinant-, phosphorylated-, and PHF-tau in solution- and solid phase BLI assays. **a-i.** Solution phase: sdAbs were loaded onto Ni-NTA biosensors to determine their affinity (K_D) for different tau preparations in solution. K_D values were determined by measuring association and dissociation with increasing concentration of the tau protein **a-c.** 2B8 sdAb had the highest affinity of the three sdAbs for recombinant tau (rec-tau) ($K_D = 39.7$ nM, 14.2 nM, and 59.8 nM for 1D9, 2B8, and tau polyclonal sdAbs, respectively). **d-f.** The three sdAbs had similar affinity for phosphorylated tau (p-tau) ($K_D = 33.4$ nM, 32.9 nM, and 32.6 nM). **g-i.** 1D9 (25.0 nM) and tau polyclonal sdAbs (43.4 nM) had 5.7- and 3.2- fold stronger affinity for PHF-tau compared to 2B8 (141.5 nM). **j-l.** Solid phase: Sensors were loaded with biotinylated rec-tau to determine the affinities of the sdAbs for tau in solid phase. K_D values were determined by measuring association and dissociation with increasing concentration of sdAb. 1D9 and 2B8 sdAbs had similar affinity for rec-tau (50.8 nM and 49.3 nM), with the tau polyclonal having approximately 2-fold lower binding (108.1 nM). sdAb binding to rec-tau was 1-3 fold lower in the solid phase than in solution.

tau levels that were normalized to NeuN levels to account for decreased cell area and numbers. As stated in Methods, in cases where two NeuN bands were visible in the blot, both bands were quantified.

We have previously shown that PHF-induced increase in total tau is also seen for phospho-tau and that antibody-mediated prevention of these increases goes hand-in-hand.^{32,33}

PHF + Ab paradigm

LDH levels: With the PHF + Ab dosing approach, the groups differed significantly in their media LDH levels ($p < 0.0001$, one-way ANOVA, [Figure 2a](#)). PHF alone increased LDH compared to untreated controls from the same plate (126% control values, $p < 0.0001$). Co-incubation with 1D9, 2B8, or poly sdAbs blocked the PHF-induced toxicity and those samples had LDH levels similar to control values (101, 96 and 95% of controls, $p = 0.009$, 0.0015 , and 0.0004 relative to PHF alone, [Figure 2a](#)).

NeuN levels: Likewise, the groups differed significantly in their NeuN levels ($p < 0.0001$, one-way ANOVA, [Figure 2b, c](#)). PHF alone induced significant toxicity (53% of controls, $p < 0.0001$). The 1D9, 2B8 and poly sdAbs prevented this toxicity resulting in NeuN levels significantly higher than in the PHF alone group (97, 102, and 123% of controls, $p = 0.0006$, 0.0001 and < 0.0001 , respectively).

Total tau: In the co-incubation approach, the groups differed significantly in their tau levels ($p < 0.0001$, one-way ANOVA), with PHF alone samples having increased intracellular tau relative to untreated controls (tau/NeuN 1.88-fold control values, $p = 0.0001$, [Figure 2b, d](#)). 1D9, 2B8, and poly sdAbs prevented the seeding induced by exogenous tau (tau/NeuN 1.08-, 0.99-, and 0.75-fold controls, $p = 0.002$, 0.0006 , and < 0.0001 respectively).

PHF → Ab paradigm

LDH levels: The same pattern of results was seen in the media from PHF → Ab cultures with the groups differing significantly ($p = 0.0002$, one-way ANOVA [Figure 2e](#)). Samples exposed to PHF alone had significantly elevated LDH relative to untreated samples from the same plate (143% of controls, $p = 0.0004$). As in the co-incubation condition, 2B8 and poly sdAbs prevented PHF-induced cell death (110 and 100% of controls, $p = 0.02$ and 0.001 relative to PHF alone).

NeuN levels: There was also a significant overall treatment effect in the PHF → Ab paradigm ($p < 0.0001$, one-way ANOVA, [Figure 2f, g](#)). Neurons incubated with PHF alone had significantly reduced NeuN levels after seven days (57% of controls, $p = 0.0002$). 1D9, 2B8, and poly sdAbs prevented this toxicity when added 24 h after the pathological tau (141, 165, and 112% of controls, $p < 0.0001$, < 0.0001 , and 0.0038 respectively).

Total tau: In the PHF pre-incubation approach, the groups also differed significantly ($p = 0.0002$, one-way ANOVA, [Figure 2f, h](#)). The PHF alone group had significantly increased tau levels compared to untreated controls (tau/NeuN 2.07-fold controls, $p = 0.0014$). As in the other dosing paradigm, all three sdAbs significantly lowered intracellular total tau levels compared to the PHF alone group (tau/NeuN 0.85-, 0.77-, and 0.84-fold

controls, $p = 0.005$, 0.003 , and 0.003 for 1D9, 2B8 and poly sdAb, respectively).

These results show that the two sdAbs selected for purification and testing, 1D9 and 2B8, bind to tau, are not toxic, and prevent PHF-induced toxicity and tau seeding in neuronal cultures. Thus, these sdAbs are well suited to address if/how antibody subclass influences efficacy. Hence, these two sdAbs were used to generate whole IgGs with identical variable regions but differing subclasses as described below.

1D9 and 2B8 subclasses bind to different forms of tau

Solution phase: In these experiments, all of the whole IgG subclasses showed apparent greater affinity for tau than their sdAbs. This is due to the overall increased avidity for tau in solution, which can be explained by the addition of a second binding site and bivalent target engagement. Specifically for rec-tau, 1D9 IgG1 (4.2 nM), IgG2A (5.1 nM) and IgG2B (10.3 nM) exhibited 9.6-, 7.8- and 3.9-fold stronger avidity compared to 1D9 sdAb ([Figure 3a-c](#)). Likewise, 2B8 IgG1 (3.0 nM), IgG2A (3.4 nM), and IgG2B (2.5 nM) had avidities 4.7-, 4.2- and 5.8-fold higher than the 2B8 sdAb ([Figure 3d-f](#), see Supplemental Table 2 for all K_D , K_{on} , and K_{off} values).

This was also the case for binding to p-tau. 1D9 IgG1 (9.1nM), IgG2A (11.0 nM) and IgG2B (10.0 nM) exhibited 3.6-, 3.0- and 3.3-fold stronger avidity compared to 1D9 sdAb (Supplemental Table 2, [Figure 3g-i](#)). Similarly, 2B8 IgG1 (8.3 nM), IgG2A (6.8 nM) and IgG2B (11.2 nM) showed 4.0-, 4.8- and 2.9-fold stronger avidities compared to 2B8 sdAb (Supplemental Table 2, [Figure 3j-l](#)).

The same avidity increase was also seen for PHF-tau binding. 1D9 IgG1 (8.9 nM), IgG2A (8.4 nM) and IgG2B (13.5 nM) exhibited 2.8-, 3.0- and 1.9-fold stronger avidity compared to 1D9 sdAb (Supplemental Table 2, [Figure 3m-o](#)). Correspondingly, 2B8 IgG1 (14.2 nM), IgG2A (69.6 nM) and IgG2B (51.0 nM) showed 10.0-, 2.0- and 2.8-fold stronger avidities compared to 2B8 sdAb (Supplemental Table 2, [Figure 3p-r](#)).

As stated in the Methods section, IgG3 did not bind to the Fc AMC biosensors so its avidity for the tau solution targets could not be established.

Solid phase: Sensors loaded with biotinylated rec-tau were reacted with increasing concentrations of the 1D9 and 2B8 whole IgGs. Interestingly, 1D9 and 2B8 subtypes did not bind more strongly to rec-tau in the solid phase compared to their sdAbs, despite the bivalent target engagement, in contrast to their solution phase avidity. 1D9 IgG1, IgG2A, IgG2B, and IgG3 yielded K_D values of 26.0 nM, 39.1 nM, 33.1 nM and 55.5 nM, respectively ([Figure 4a-d](#), see Supplemental Table 3 for all K_D , K_{on} , and K_{off} values). The range was comparable for the 2B8 subtypes, resulting in K_D values of 37.0 nM, 47.3 nM, 51.9 nM and 53.3 nM for IgG1, IgG2A, IgG2B and IgG3, respectively (Supplemental Table 3, [Figure 4e-h](#)).

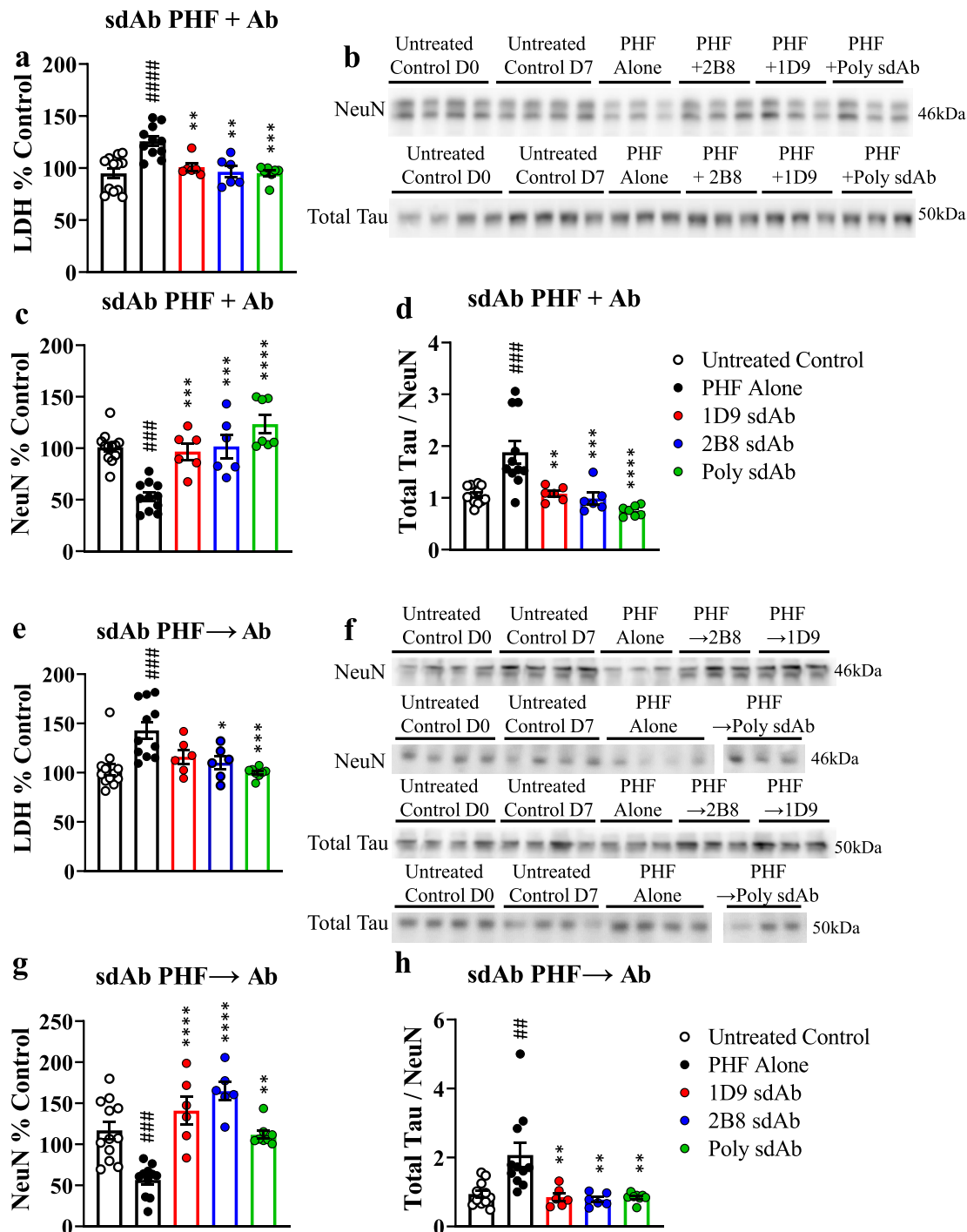


Figure 2. 1D9, 2B8 and tau polyclonal sdAbs prevent PHF-induced toxicity and seeding in neuronal cultures. JNPL3 primary neurons were incubated with 1 μ g/ml human derived PHF and 1D9, 2B8 or polyclonal (poly) sdAb using the PHF + Ab and PHF \rightarrow Ab dosing paradigms for 7 days (n = at least 6 replicates per condition). **a.** PHF alone increased LDH levels in media from cultures treated with the PHF + Ab paradigm, (126% of untreated control, $p < 0.0001$, overall $p < 0.0001$, one-way ANOVA). Addition of the 1D9, 2B8, and tau poly sdAbs blocked this toxicity (101, 96 and 95% of control, $p = 0.009$, 0.0015, and 0.0004 relative to PHF alone). **b.** Immunoblots showing NeuN and total tau levels in treated JNPL3 cell lysate. **b, c.** In the PHF + Ab group there was less NeuN in the samples from PHF alone treated cells (53% of control, $p < 0.0001$, overall $p < 0.0001$, one-way ANOVA). All three sdAbs prevented this toxicity and had higher NeuN levels compared to PHF alone (97, 102, and 123% of control, $p = 0.0006$, 0.0001 and

1D9 IgG2B shows increased solid phase binding by ELISA compared to other subclasses

Solid phase binding was further tested using two different ELISA protocols. The first assay followed standard solid phase ELISA methods, where plates were coated with the same soluble PHF used in the culture efficacy experiments, as well as the sarkosyl soluble and insoluble fractions prepared from the same tissue. The insoluble fraction differs from the PHF used in the cultures as it has not been dialyzed or boiled to resolubilize the smaller aggregates. The second assay was a competition ELISA where the antibodies were pre-incubated with increasing concentrations of soluble PHF before being added to the assay plate. Binding to the soluble fraction rather than plate bound tau correlated with tau antibody efficacy in both of our previous reports using culture and in vivo models.^{32,33}

Interestingly, 1D9 IgG2B had significantly higher binding to plate bound PHF-tau compared to the other subtypes at dilutions from 1/40 through 1/25000 (*p* values from 0.03 to < 0.0001, two-way ANOVA, Figure 4i). Similar results were seen with the sarkosyl insoluble and sarkosyl soluble fractions bound to the plate (Figure 4j, k). Binding to sarkosyl insoluble tau was significantly higher with 1D9 IgG2B than the other subtypes from dilutions 1/40 through 1/5000 (*p* values from 0.03 to < 0.0001, two-way ANOVA, Figure 4j). Using sarkosyl soluble tau, 1D9 IgG2B had significantly higher binding at 1/40 (*p* < 0.0001 for all, two-way ANOVA, Figure 4k) and at 1/200 (*p* = 0.0004 to < 0.0001, Figure 4k) and at 1/1000 (*p* = 0.013 and 0.004, Figure 4k).

A single concentration of antibody was then chosen for a competitive ELISA to determine if 1D9 subtype binding to soluble PHF-tau differed. Subtypes were incubated with increasing concentrations of PHF (0 – 200 ng) before being added to the PHF-coated assay plate. 1D9 IgG1, IgG2A and IgG2B had significantly reduced binding to the plate following pre-incubation with soluble PHF-tau (Figure 4l). Specifically, 1D9 IgG1 showed decreased binding to the plate at the two highest PHF concentrations (*p* = 0.03, < 0.0001,

two-way ANOVA, Figure 4l), compared to the no PHF control. Likewise, plate binding was significantly reduced for 1D9 IgG2A at the three highest PHF pre-incubation concentrations (*p* = 0.013, 0.004 and 0.0014, Figure 4l). Similarly, IgG2B had decreased binding at the two highest PHF concentrations (*p* = 0.03, 0.012, Figure 4l).

1D9 subclasses are not toxic in mixed neuron/glia tauopathy cultures, whereas 2B8 subclasses are toxic under these conditions

Antibody effector functions are to a large extent mediated by other cell types than neurons, in particular microglia, and vary by subtype. Therefore, the comparison of potential toxicity and efficacy of the different subtypes was conducted in primary cortical cultures that contain all cell types, hereafter referred to as mixed cortical cultures. These cultures were prepared from JNPL3 tauopathy neonates and incubated with 10 µg/ml of each antibody subtype (IgG1, 2A, 2B and 3) for 96 hours. Media and cell lysate were then collected for LDH and NeuN immunoblotting. In mixed cultures, a higher dose of PHF-tau (10 µg/ml) is needed for toxicity than in neurons (1 µg/ml) and, therefore, correspondingly higher dose of antibody to block the effect.

LDH levels: In media collected from 1D9 subtype treated samples there were no significant differences compared to untreated control samples, or between subtypes, Figure 5a). For cells incubated with 2B8 subtypes, there was a significant overall treatment effect (*p* = 0.003, one-way ANOVA, Figure 5b). 2B8 IgG2A, IgG2B and IgG3 had significantly elevated LDH levels in the culture media relative to the untreated samples (206, 196, and 176% control values, *p* = 0.002, 0.006, 0.046, Figure 5b). IgG1 values showed a trend towards increased LDH but were not significant (*p* = 0.07).

NeuN levels: Similarly, NeuN levels in cells exposed to 1D9 subtypes were not altered compared to controls (Figure 5c, d). However, in samples incubated with the 2B8 subtypes, NeuN levels were overall significantly reduced when examined at 96 h (*p* < 0.0001, one-way ANOVA), and specifically for IgG1, 2A, 2B and 3 to 48,

< 0.0001, respectively). **b, d.** PHF alone increased intracellular tau relative to untreated samples (ratio tau/NeuN 1.88, *p* = 0.0001, overall *p* < 0.0001, one-way ANOVA). 1D9, 2B8, and tau poly sdAbs prevented this increase (ratio tau/NeuN 1.08, 0.99, and 0.75, *p* = 0.002, 0.0006, and < 0.0001 respectively). **e.** In PHF → Ab cultures, PHF alone increased LDH relative to untreated samples (143% of control, *p* = 0.0004, overall *p* value = 0.0002, one-way ANOVA). 2B8 and tau poly sdAbs prevented the PHF-induced increase (110 and 100% of control, *p* = 0.02 and 0.001 relative to PHF alone). **f.** Immunoblots showing NeuN and total tau levels in treated JNPL3 cell lysate. **f, g.** Samples incubated with PHF alone had significantly reduced NeuN levels in the PHF → Ab paradigm as well (57% of control, *p* = 0.0002, overall *p* < 0.0001, one-way ANOVA). When added 24 h after PHF, 1D9, 2B8, and tau poly sdAbs prevented PHF toxicity (141, 165, and 112% of control, *p* < 0.0001, < 0.0001, and 0.0038 respectively). **f, h.** In the PHF → Ab paradigm, PHF alone increased intracellular tau (ratio tau/NeuN 2.07, *p* = 0.0014, overall *p* = 0.0002, one-way ANOVA). Samples treated with all three sdAbs had lower intracellular total tau than those given exogenous PHF alone (ratio tau/NeuN 0.85, 0.77, and 0.84, *p* = 0.005, 0.003, and 0.003 for 1D9, 2B8 and tau poly sdAbs, respectively).

Bars represent average ± SEM.

p ≤ 0.01, ### *p* ≤ 0.001, * *p* ≤ 0.05, ** *p* ≤ 0.01, *** *p* ≤ 0.001, **** *p* < 0.0001.

significant compared to untreated control, * significant compared to PHF alone.

Solution phase BLI binding assay- sdAb isotypes

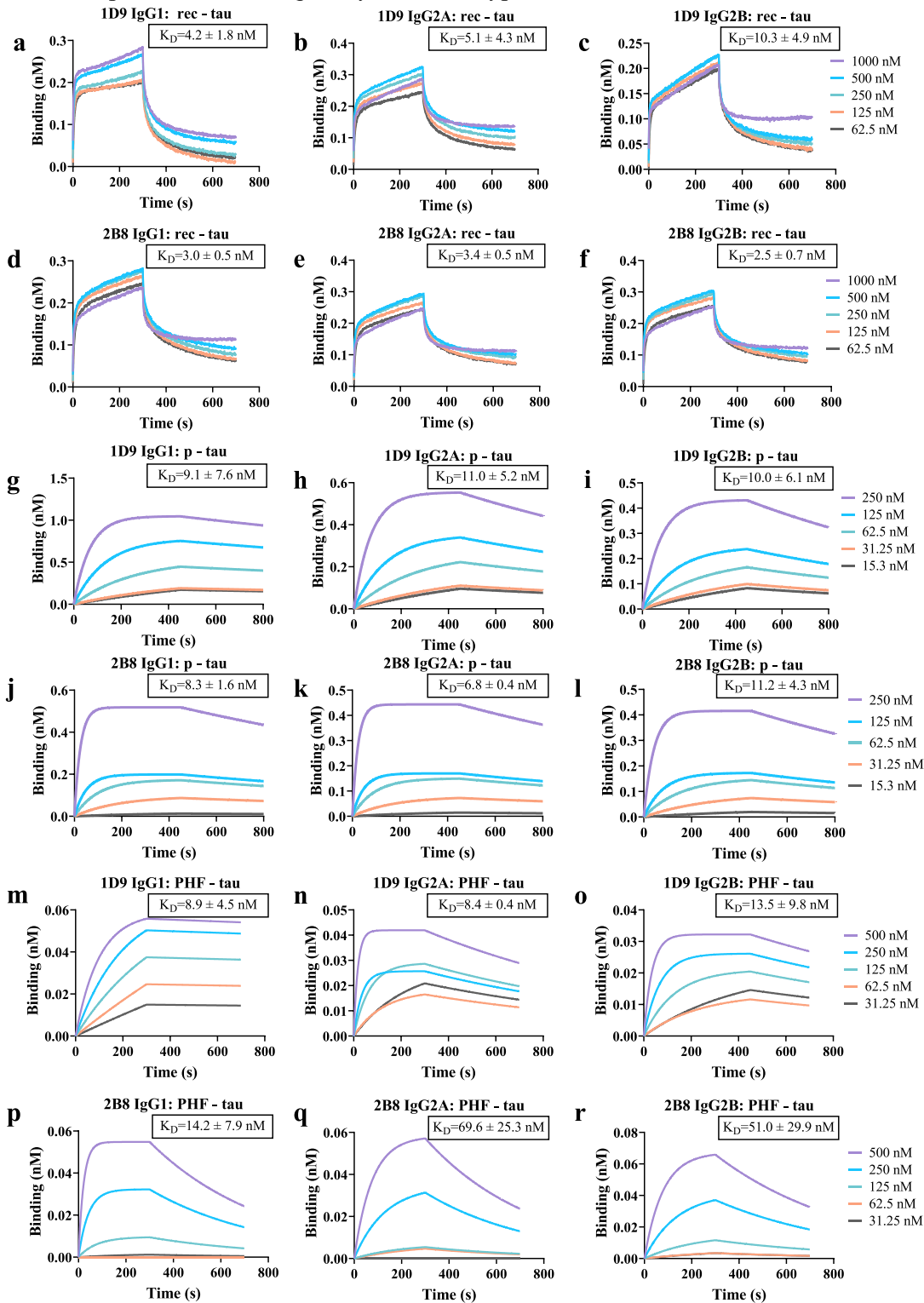


Figure 3. 1D9 and 2B8 IgG subclasses bind recombinant-, phosphorylated-, and PHF-tau in solution phase BLI assay. Whole IgG subclasses (Fc-(sdAb)₂) were loaded onto Anti-Mouse IgG Fc Capture (AMC) biosensors. K_D values were determined using increasing concentration of recombinant- (rec-tau), phosphorylated- (p-tau), and PHF-tau. The IgG subclasses displayed an apparent

48, 37 and 46% of untreated control, respectively ($p \leq 0.0001$ for all, [Figure 5c, e](#)).

2B8 toxicity is dependent on the presence of pathological tau

The toxicity seen when using IgG subclasses of 2B8 was somewhat surprising given the lack thereof for the unmodified 2B8 sdAb. We hypothesize that the addition of a second binding site allows 2B8 to bind to and stabilize a toxic tau conformer. JNPL3 cells overexpress mutant tau that is prone to aggregation, leading to neurotoxicity. Thus, the cultures already contain some pathological misfolded tau protein. If 2B8 binds to that misfolded tau and stabilizes it, the concentration of that conformer would increase leading to toxicity. In this scenario, the 2B8 subclasses would not be toxic in wild-type mouse neurons that only contain normal mouse tau protein, which is not toxic. To assess this, we incubated mixed cultures prepared from wild type animals expressing only the three normal mouse tau isoforms with 10 $\mu\text{g/ml}$ of 2B8 IgG1, IgG2A, IgG2B, and IgG3 for up to 6 days. Lysates were probed for NeuN levels and media for LDH, and no changes were seen with any of the antibodies, indicating lack of toxicity of the 2B8 subtypes in these cells ([Figure 5f-h](#)). These findings confirm our hypothesis that the toxicity of the 2B8 subtypes likely relates to their ability to stabilize misfolded toxic tau protein, when both arms of the antibody interact with pathological tau.

1D9 IgG1 and IgG2A are most effective in preventing PHF-induced toxicity and seeding, whereas 2B8 subclasses are either ineffective or further promote toxicity

The antibodies were then tested for efficacy using the PHF + Ab and PHF \rightarrow Ab dosing conditions. Mixed cortical cultures were incubated with 10 $\mu\text{g/ml}$ each of the human-derived PHF-tau and each subclass and collected 96 h after the last treatment. In addition, untreated control cells were collected both prior to treatment, and after 96 h incubation to control for any changes that occur normally in culture. Toxicity was assessed using two different methods, immunoblotting for NeuN and LDH levels in the culture media. We then assayed total and phospho-tau levels in these same

samples to determine whether 1D9 and 2B8 could prevent pathological tau seeding. As above, values were normalized using NeuN.

PHF + Ab paradigm

LDH levels: A significant treatment effect was detected in the 1D9 group ($p = 0.006$, one-way ANOVA). PHF alone significantly increased LDH levels in the media compared to media from untreated control cells (137% control values, $p = 0.05$, [Figure 6a](#)). Cultures treated with both PHF and either 1D9 IgG1, 2A or 2B showed no such increase relative to controls. However, 1D9 IgG3 failed to prevent the PHF-induced cell death (154% control values, $p = 0.01$, [Figure 6a](#)).

Likewise, a significant treatment effect was seen in the 2B8 group ($p < 0.0001$, one-way ANOVA, [Figure 6b](#)). However, in stark contrast to the 1D9 subclasses, 2B8 IgG2A, IgG2B, and 3 were highly toxic compared to untreated control cells, with IgG2B and IgG3 also significantly elevated compared to those treated with PHF alone (279, 390, and 293% control values, vs Untreated $p = 0.001$, 0.0001 , and 0.0011 , vs PHF $p < 0.0001$, 0.04 , [Figure 6b](#)).

NeuN levels: Cell lysate was also collected from those same cultures and probed for NeuN levels ([Figure 6c](#)), resulting in a 1D9 subtype treatment effect ($p < 0.0001$, one-way ANOVA). PHF alone induced significant toxicity in the cells after 96 h (56 % of control values, $p < 0.0001$, [Figure 6d](#)). Subtypes IgG1 and IgG2A prevented the PHF-induced toxicity (115 and 112% of control values, $p < 0.0001$ for both, compared to PHF alone, [Figure 6d](#)), while IgG2B and 3 did not.

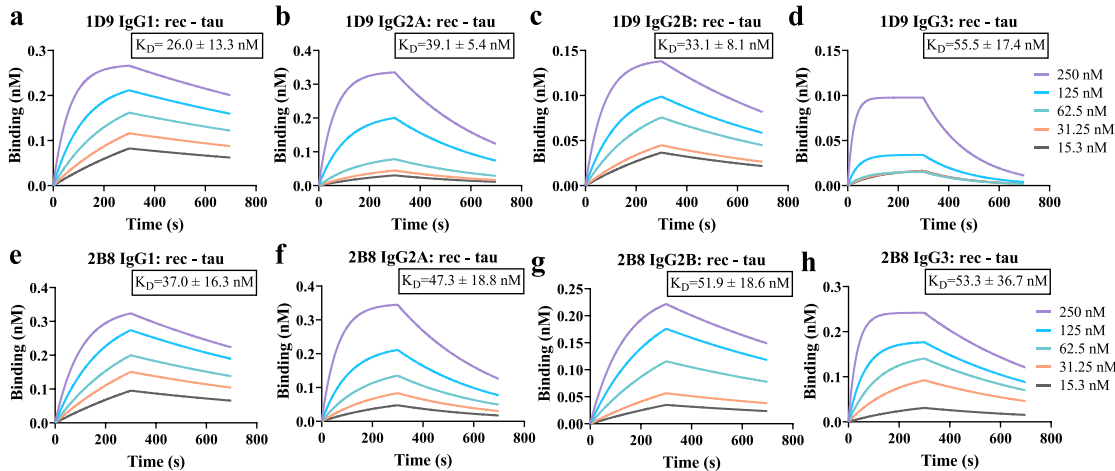
Although there was also a significant overall treatment effect with 2B8 ($p < 0.0001$, one-way ANOVA), none of the subtypes prevented the PHF-induced toxicity, and some added to its toxicity. PHF alone again significantly decreased NeuN levels (50% of control, $p < 0.0001$, [Figure 6c, e](#)). All four 2B8 subtypes significantly lowered NeuN levels compared to untreated control (38, 25, 17 and 25% of control, $p < 0.0001$ for all, [Figure 6e](#)). Further, 2B8 IgG2A, IgG2B and IgG3 groups had lower NeuN levels than the PHF alone group ($p = 0.03$, 0.001 and 0.05).

Total tau: Quantitation of immunoblots from the PHF + Ab paradigm showed an overall treatment effect on total tau levels in cultures treated with 1D9 subtypes

increased affinity for tau relative to their sdAbs. This results from increased avidity because of bivalent target engagement. **a-c**. 1D9 IgG1, IgG2A, and IgG2B had 9.6, 7.8-, and 3.9-fold stronger avidity for rec-tau compared to 1D9 sdAb ($K_D = 4.2$ nM, 5.1 nM, and 10.3 nM, respectively). **d-f**. 2B8 IgG1, IgG2A, and IgG2B had 4.7-, 4.2- and 5.8-fold higher avidity than the sdAb for rec-tau ($K_D = 3.0$ nM, 3.4 nM, and 2.5 nM, respectively). **g-i**. For p-tau, whole 1D9 IgGs had 3 – 3.6 fold higher avidity relative to their sdAb ($K_D = 9.1$ nM, 11.0 nM, and 10.0 nM for IgG1, IgG2A, and IgG2B, respectively). **j-l**. The effect of bivalent engagement was also seen with 2B8 in assays with p-tau as IgG1 (8.3 nM), IgG2A (6.8 nM), and IgG2B (11.2 nM) had 4.0-, 4.8-, and 2.9-fold stronger avidity compared to the 2B8 sdAb. **m-o**. When tested against human derived PHF, 1D9 IgG1, IgG2A, and IgG2B exhibited 2.8-, 3.0-, and 1.9-fold stronger avidity compared to 1D9 sdAb ($K_D = 8.9$ nM, 8.4 nM, and 13.5 nM, respectively). **p-r**. K_D values for 2B8 IgG subclasses were also higher for PHF than their sdAb (14.2 nM, 69.6 nM, and 51.0 nM, for IgG1, IgG2A and IgG2B, respectively).

* Due to low Fc binding IgG3 subtypes did not yield results in these tests.

Solid phase BLI binding assay- sdAb isotypes



ELISA binding assay- 1D9 isotypes

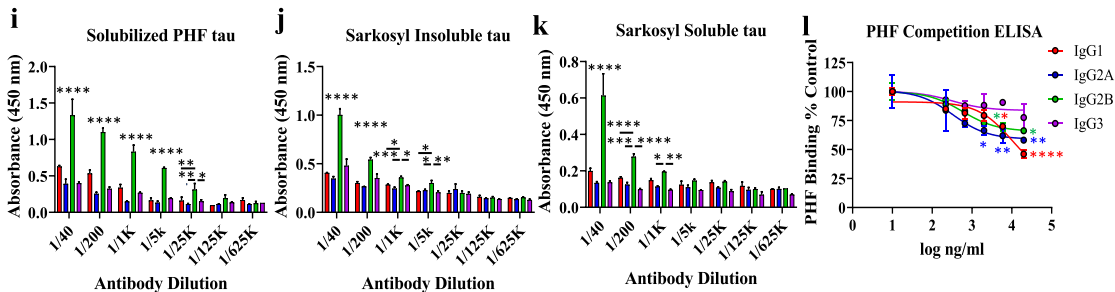


Figure 4. 1D9 and 2B8 IgG subclasses bind recombinant tau in solid phase BLI assay; 1D9 IgG2B has highest affinity of the subclasses for tau in solid phase ELISA. Only the IgG3 subclass of 1D9 does not bind to PHF-tau in solution. **a-h.** In the BLI experiments, biosensors were loaded with biotinylated recombinant tau (rec-tau). Association and dissociation of increasing concentrations of whole IgG subtypes were measured and K_D values determined. Interestingly, there was no major increase in avidity over the unmodified 1D9 and 2B8 sdAbs despite the presence of two binding sites on the whole IgG. **a-d.** 1D9 subtypes IgG1, IgG2A, IgG2B, and IgG3 had similar K_D values (26.0 nM, 39.1 nM, 33.1 nM, and 55.5 nM) that were comparable to 1D9 sdAb ($K_D = 50.8$ nM, see Figure 1j). **e-h.** 2B8 subtypes also had similar K_D values (37.0 nM, 47.3 nM, 51.9 nM, and 53.3 nM for 2B8 IgG1, IgG2A, IgG2B, and IgG3) that were comparable to 2B8 sdAb ($K_D = 49.3$ nM, see Figure 1k). For the standard ELISA, plates were coated with solubilized PHF, sarkosyl insoluble, and sarkosyl soluble tau fractions (1 μ g per well). Plates were blocked and then incubated for 3 h with serial dilutions of each 1D9 subtype. **i.** IgG2B had significantly higher binding than the other subclasses to PHF-tau from 1/40 through 1/25000 (p values from 0.03 to < 0.0001 , two-way ANOVA). **j.** For sarkosyl insoluble tau, 1D9 IgG2B binding was significantly higher than the other subtypes from dilutions 1/40 through 1/5000 (p from 0.03 to < 0.0001 , two-way ANOVA). **k.** On plates coated with sarkosyl soluble tau, 1D9 IgG2B had significantly higher binding at 1/40 ($p < 0.0001$ for all, two-way ANOVA) and at 1/200 ($p = 0.0004$ to < 0.0001 for all) and at 1/1000 ($p = 0.013$ and 0.004 relative to IgG2A and IgG3). **l.** For the competitive ELISA, plates were coated with solubilized PHF-tau and a single concentration of each of the 1D9 IgG subclass was pre-incubated with increasing concentrations of PHF-tau before adding it to the wells. 1D9 IgG1 had decreased binding to the plate at the two highest PHF concentrations ($p = 0.03$, < 0.0001 , two-way ANOVA) compared to the no PHF control. Plate binding was significantly reduced for 1D9 IgG2A at the three highest PHF pre-incubation concentrations ($p = 0.013$, 0.004, 0.0014). IgG2B had decreased binding at the two highest PHF concentrations as well ($p = 0.03$, 0.012). There was no change with IgG3, indicating that it did not bind to PHF-tau in solution.

Bars represent average \pm SEM.

* $p \leq 0.05$, ** $p \leq 0.01$, **** $p < 0.0001$, compared to 1D9 IgG2B in panels i-k, and relative to samples receiving no PHF pre-incubation in panel l.

and PHF ($p < 0.0001$, one-way ANOVA, Figure 6f, g). PHF alone induced seeding in the cultures after 96 h (tau/NeuN = 1.94-fold, $p = 0.0004$, Figure 6g). IgG1 and IgG2A prevented the increased intracellular tau

levels (tau/NeuN = 0.87 and 0.75 of untreated control, $p = 0.0016$ and 0.0003, compared to PHF alone, Figure 6g). Similar to the toxicity experiments, IgG2B and IgG3 had no effect.

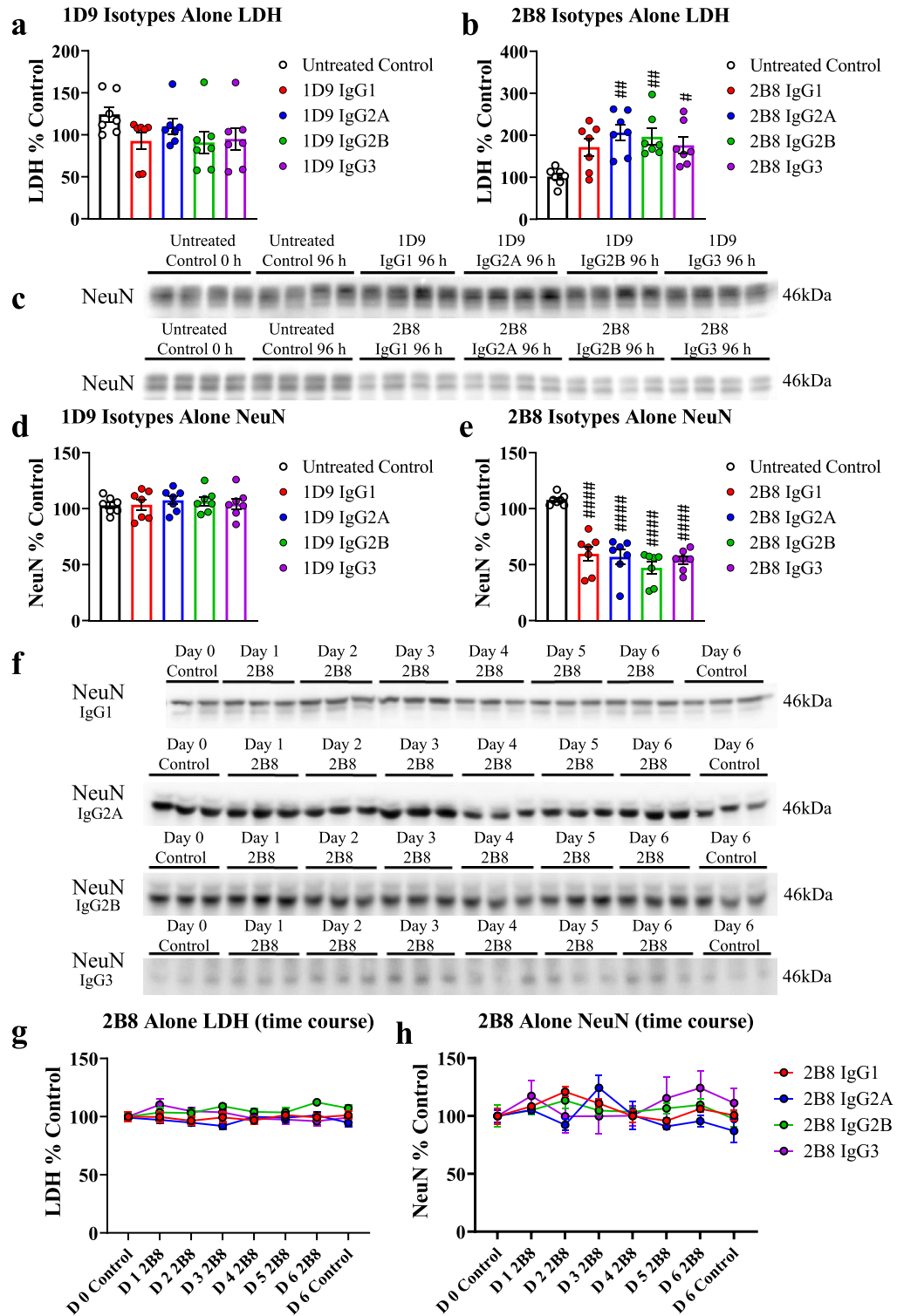


Figure 5. 1D9 subclasses are not toxic in mixed neuron/glia cultures while 2B8 subclasses display toxicity that is dependent on the presence of pathological tau. **a-e.** Mixed neuron/glia cultures prepared from JNPL3 mice were incubated with 1D9 and 2B8 subtypes alone (10 μ g/ml) for 96 h (n = at least 6 replicates per condition). **a.** There was no significant change in LDH levels in cultures treated with any of the 1D9 subtypes. **b.** Incubation with 2B8 IgG2A, IgG2B and IgG3 alone increased LDH relative to

An overall treatment effect was also observed in culture treated with 2B8 subtypes and PHF ($p = 0.0002$, one-way ANOVA, [Figure 6f, h](#)). PHF alone samples had increased intracellular tau levels relative to untreated samples after 96 h ($\text{tau/NeuN} = 1.91$, $p = 0.017$). In contrast to the 1D9 subtypes, none of the 2B8 subtype treated cells had total tau levels lower than PHF alone, and indeed those treated with IgG3 were significantly higher compared to both untreated and PHF alone cells ($\text{tau/NeuN} = 3.81$, $p < 0.0001$ and $= 0.0093$ respectively, [Figure 6h](#)).

Phospho-tau: We also probed lysates for tau phosphorylated at Ser199 (pSer199, [Figure 6i](#)). As with total tau, a significant overall treatment effect was observed on pSer199 ($p < 0.0001$, one-way ANOVA) in cells incubated with PHF with or without the 1D9 subtypes ([Figure 6j](#)). Addition of PHF increased intracellular phospho-tau relative to untreated controls (pSer199/NeuN = 2.28, $p = 0.0003$, [Figure 6j](#)). Again, IgG1 and IgG2A prevented this increase (pSer199/NeuN = 0.84 and 0.86 of untreated control, $p = 0.0012$ and 0.0015 , compared to PHF alone, [Figure 6j](#)).

Similar to their effects on total tau, the IgG2A, IgG2B and IgG3 subtypes of 2B8 led to higher levels of pSer199 tau than either untreated controls or cells exposed to PHF alone (pSer199/NeuN = 4.26, 4.57 and 4.50-fold untreated control, $p = 0.0005$, $= 0.0001$ and $= 0.0006$, relative to untreated samples, $p = 0.047$, $= 0.013$, $= 0.040$, relative to PHF alone, overall $p < 0.0001$, one-way ANOVA, [Figure 6i, k](#)).

PHF → Ab paradigm

As detailed above, this paradigm requires antibody uptake into neurons for efficacy.

LDH levels: In cells treated with PHF and 1D9 subtypes an overall treatment effect was seen on LDH levels ($p = 0.0002$, one-way ANOVA, [Figure 7a](#)). LDH was increased in cells treated with PHF alone, or PHF followed by 1D9 IgG2B (177% of control, $p = 0.02$), which was not blocked by 1D9 IgG2B (208% of control, $p = 0.0008$, [Figure 7a](#)). 1D9 IgG1 treated cells had significantly lower LDH compared to PHF alone (108% control values, $p = 0.05$).

Likewise, with this dosing approach, there was also an overall treatment effect on LDH in the 2B8 subtype group ($p < 0.0001$, one-way ANOVA, [Figure 7b](#)). However, in contrast to the beneficial effects of most of the 1D9

subtypes, most of the 2B8 subtypes enhanced PHF-induced toxicity instead of preventing it. Media from cells incubated with PHF and 2B8 IgG1, 2A and 2B had elevated LDH levels compared to untreated samples (187, 214, 248% control values, $p = 0.009$, $= 0.0002$, < 0.0001 , [Figure 7b](#)). Those treated with PHF and 2B8 IgG 2A and 2B were also elevated compared to PHF alone ($p = 0.05$, 0.0004).

NeuN levels: Immunoblotting for NeuN was then conducted on cell lysate from these same cultures ([Figure 7c](#)). There was a significant overall effect of PHF and 1D9 treatment ($p < 0.0001$, one-way ANOVA). PHF alone induced significant toxicity in the treated cells (43% of control, $p < 0.0001$, [Figure 7d](#)). 1D9 IgG1, IgG2A, and IgG2B treated cells had significantly higher NeuN levels compared to PHF alone (86, 100, and 65 % of untreated control, $p < 0.0001$, < 0.0001 and $= 0.04$, respectively, [Figure 7d](#)).

In contrast, none of the 2B8 subclasses prevented the PHF-induced toxicity, although there was a significant overall effect of the PHF and 2B8 treatment ($p < 0.0001$, one-way ANOVA). Specifically, PHF alone was toxic (62 % of untreated control, $p < 0.0001$, [Figure 7e](#)), and all the 2B8 subtype groups had reduced NeuN relative to untreated control cells (55, 77, 42 and 34 % of control, $p < 0.0001$, $= 0.04$, < 0.0001 and < 0.0001 , respectively, [Figure 7e](#)).

Total tau: Both antibody and subclass impacted efficacy in the PHF → Ab dosing condition as well. As above, blots were probed for total tau and the values corrected for NeuN levels ([Figure 7f](#)). An overall significant treatment effect was seen in the 1D9 group ($p < 0.0001$, one-way ANOVA, [Figure 7g](#)). Samples exposed to PHF alone had significantly increased intracellular tau levels (tau/NeuN ratio = 1.96, $p < 0.0001$, [Figure 7g](#)). The IgG1, IgG2A and IgG2B subtypes of 1D9 prevented tau seeding in this treatment paradigm ($\text{tau/NeuN} = 1.05$, 0.97, and 1.39, $p < 0.0001$ compared to PHF alone for all, [Figure 7g](#)).

An overall significant effect was also observed in the cultures incubated with PHF and 2B8 using this dosing method ($p = 0.0003$, one-way ANOVA). PHF alone induced a significant increase in total tau in the cells ($\text{total tau/NeuN} = 1.47$, $p = 0.016$, [Figure 7h](#)). In contrast to the 1D9 subtypes, 2B8 IgG1, IgG2B and IgG3 also showed elevated total tau levels following PHF exposure ($\text{total tau/NeuN} = 1.55$, 1.68 and 1.61 $p = 0.013$, $= 0.0015$ and $= 0.013$, relative to untreated

untreated controls (206, 196, and 176% of control values, $p = 0.002$, 0.006, 0.046, overall $p = 0.003$ one-way ANOVA). There was also a strong trend towards increased LDH with 2B8 IgG1 ($p = 0.07$) **c**. Immunoblots showing NeuN levels in treated JNPL3 cell lysates. **d**. None of the 1D9 subtypes altered NeuN levels relative to untreated controls. **e**. All 2B8 subtypes reduced NeuN levels compared to untreated cells (48, 48, 37, and 46 % of control for IgG1, 2A, 2B and 3, respectively, $p \leq 0.0001$ for all, overall $p < 0.0001$ one-way ANOVA). **f**. Immunoblots showing NeuN levels in lysates of wild-type cells from mixed neuron/glia cultures treated with 2B8 sdAb. **g-h**. There were no significant changes in LDH levels (**g**) or NeuN levels (**h**) over the 6 day treatment period in the wild-type mouse cells, indicating that the toxic effects seen in the JNPL3 cells in **b** and **e** is dependent on pathological tau.

Bars represent average \pm SEM.

$p \leq 0.05$, ### $p \leq 0.001$, ##### $p < 0.0001$, compared to untreated control.

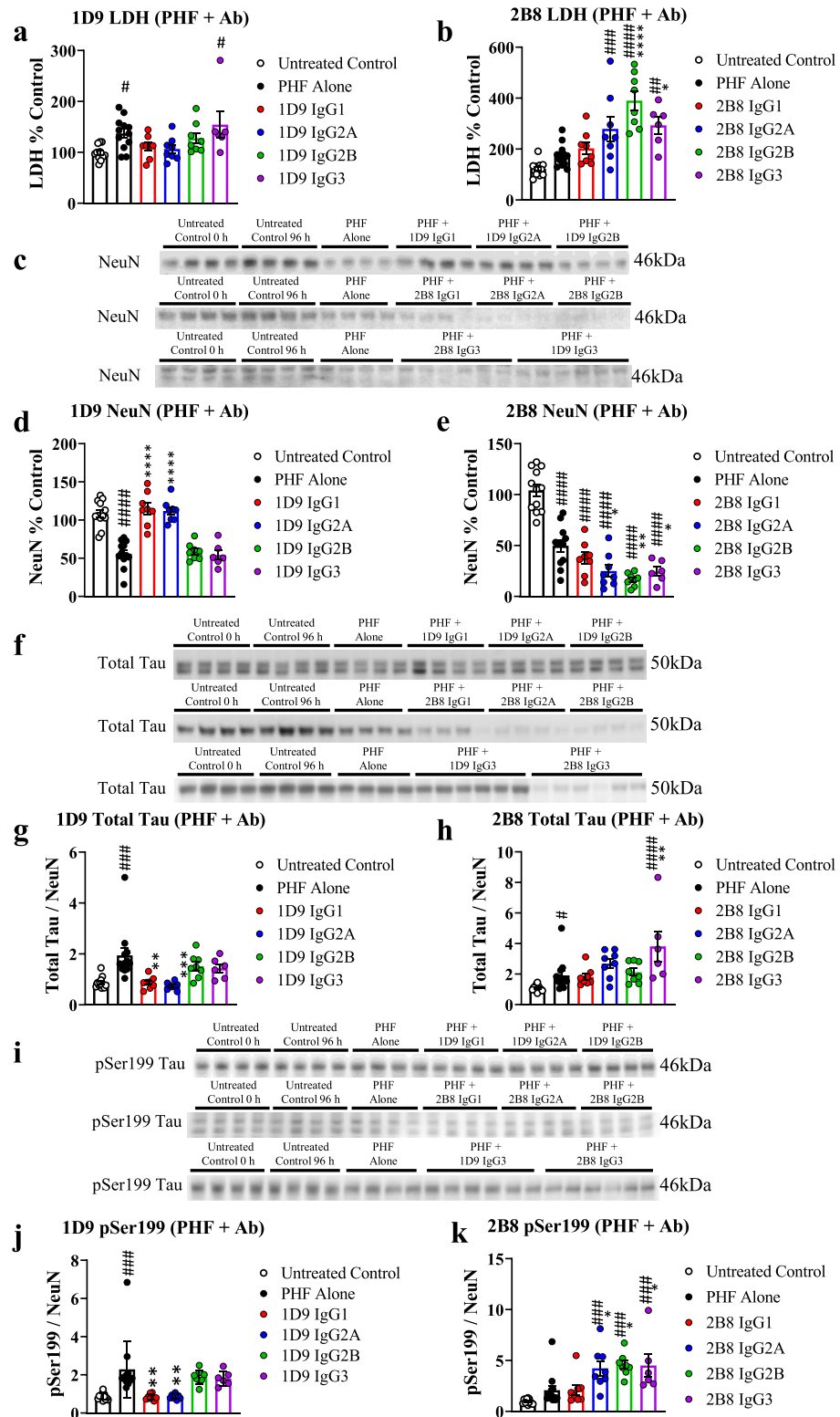


Figure 6. In the PHF + Ab paradigm, 1D9 IgG1 and IgG2A are the most efficacious subclasses in preventing PHF-induced toxicity and tau seeding, whereas all 2B8 IgG subclasses are toxic or ineffective. Mixed neuron/glia cultures prepared from JNPL3 pups were exposed to 10 µg/ml PHF and 10 µg/ml tau sAb IgG subclasses added simultaneously (PHF + Ab, n = at least 6 replicates

control, Figure 7h). None of the 2B8 subtypes had total tau levels significantly lower than PHF alone.

Phospho-tau: A similar pattern was seen when intracellular pSer199 tau was quantified (Figure 7i). In the 1D9 group, there was an overall treatment effect ($p < 0.0001$, one-way ANOVA), and PHF alone increased pSer199 tau in the cells (pSer199/NeuN = 2.76, $p < 0.0001$, Figure 7j). Treatment with the IgG1, IgG2A and IgG2B subtypes of 1D9 after PHF significantly lowered pSer199 relative to PHF alone (pSer199/NeuN ratio = 1.31, 1.03, and 1.86 of untreated control, $p < 0.0001$, < 0.0001 , and = 0.03, Figure 7j).

Likewise, in the 2B8 group, there was an overall treatment effect ($p < 0.0001$, one-way ANOVA), and PHF alone also significantly increased phospho-tau levels in the 2B8 group (pSer199/NeuN = 1.93, $p = 0.001$, Figure 7k). However, as for total tau, in contrast to the 1D9 subtypes, none of the 2B8 subtypes prevented the PHF-induced increase in pSer199 (pSer199/NeuN = 1.83, 2.11 and 2.76 of untreated control, $p = 0.013$, = 0.0005 and < 0.0001 , for IgG1, IgG2B and IgG3 subtypes, respectively, relative to untreated control, Figure 7k). None of the subtypes differed from PHF alone.

1D9 IgG3 uptake into neurons and glia is lower than for the other 1D9 subclasses

The culture experiments showed a clear difference in efficacy both between antibodies and for 1D9 in particular, between subclasses of the same antibody. 1D9 IgG1 and IgG2A showed similar efficacy in both dosing paradigms, IgG2B was only effective in the PHF → Ab condition, and IgG3 had no efficacy in either condition. We

have previously shown in the PHF → Ab paradigm that uptake into neurons is essential to prevent PHF-induced toxicity and seeding.^{32,33} Additionally, other groups have shown that clearance of extracellular tau, such as in the PHF + Ab paradigm, through microglia is subclass dependent.^{19,20,54,55} Therefore, we hypothesized that in addition to the impact of subclass on tau binding, the subclass-dependent efficacy of 1D9 may relate to differences in cellular uptake as well.

To explore this, the 1D9 subclasses were labelled with CypHer 5, a dye that fluoresces in acidic compartments like endosomes and lysosomes, allowing us to ensure that any signal seen is intracellular. We first exposed mixed cortical cultures to 5 µg/ml of the labelled antibodies for one h at 37°C alone with no exogenous PHF added. Live images of the cultures were then captured and quantified using Image J (n = 18-20 images per antibody 20x magnification, Figure 8a). Overall uptake was expressed as the total number of pixels per image positive for antibody signal. There was an overall difference in uptake between the subtypes ($p < 0.0001$, one way ANOVA). The IgG1, IgG2A, and IgG2B subtypes of 1D9 had similar degree of uptake with the antibody localized to the cell bodies. IgG3, however, had very limited cellular uptake compared to each of the other subtypes ($p < 0.0001$, Figure 8b). To determine which cell type internalized the antibodies, additional cells were fixed and stained with a total tau antibody to label neurons (Figure 8c). We then used an Image J colocalization macro to determine the colocalization of the CypHer 5 and neuronal marker. In all cases the majority of the antibody fluorescence

per condition). Cells were collected 96 h following treatment. **a.** For the 1D9 co-incubation samples, the PHF alone increased LDH levels in culture media (137% of control, $p = 0.05$, overall $p = 0.006$, one-way ANOVA). 1D9 IgG1, IgG2A and IgG2B prevented this increase but not 1D9 IgG3 (154% of control, $p = 0.01$). **b.** In the co-incubation condition, 2B8 IgG2A, IgG2B and IgG3 had higher LDH levels in the media compared to untreated samples, with IgG2B and IgG3 also significantly higher relative to PHF alone (279, 390, and 293% of control values, $p = 0.001$, 0.0001, and 0.0011 vs untreated control, $p < 0.0001$, and 0.04 vs PHF, overall $p < 0.0001$, one-way ANOVA). **c.** Immunoblots showing JNPL3 cell lysates probed for NeuN from samples treated with PHF and the IgG sAb subclasses. **d.** In the 1D9 group, PHF alone decreased NeuN in cells (56% of control, $p < 0.0001$, overall $p < 0.0001$, one-way ANOVA). 1D9 IgG1 and IgG2A prevented PHF-induced toxicity (115 and 112% of control values, $p < 0.0001$ for both), while IgG2B and 3 did not. **e.** In the 2B8 group, PHF alone decreased NeuN (50% of control, $p < 0.0001$, overall $p < 0.0001$, one-way ANOVA). None of the 2B8 IgG subtypes prevented the PHF-induced toxicity (38, 25, 17, 25 % of control, $p < 0.0001$ for all). The 2B8 IgG2A, IgG2B, and IgG3 treated samples were also reduced compared to PHF alone ($p = 0.03$, 0.001, and 0.05). **f.** Tau immunoblots of the JNPL3 lysate from the same cultures used in the LDH and NeuN quantification. Tau values in g, h, j and k were normalized using NeuN to account for cell loss or retraction. **g.** In the 1D9 group, PHF alone increased intracellular tau (ratio tau/NeuN 1.94-fold over control, $p = 0.0004$, overall $p < 0.0001$, one-way ANOVA). 1D9 IgG1 and IgG2A prevented tau seeding resulting in lower intracellular tau levels relative to PHF alone (ratio tau/NeuN 0.87 and 0.75, $p = 0.0016$ and 0.0003) while IgG2B and IgG3 had no effect. **h.** In the 2B8 group, PHF alone increased intracellular tau (tau/NeuN ratio 1.91, $p = 0.017$, overall $p = 0.0002$, one-way ANOVA), and none of the 2B8 IgG subclasses prevented tau seeding. 2B8 IgG3 resulted in higher tau levels than in both untreated control and PHF alone cells (ratio tau/NeuN 3.81, $p < 0.0001$ and = 0.0093 respectively). **i.** The same JNPL3 lysate was also immunoblotted for tau phosphorylated at Ser199. **j.** In the 1D9 group, PHF increased intracellular phospho-tau relative to untreated control (ratio pSer199/NeuN 2.28, $p = 0.0003$, overall $p < 0.0001$, one-way ANOVA). Both 1D9 IgG1 and IgG2A prevented pathological tau seeding (ratio pSer199/NeuN ratio 0.84 and 0.86, $p = 0.0012$ and 0.0015). **k.** In the 2B8 group, IgG2A, IgG2B and IgG3 treated samples all contained higher levels of pSer199 tau than either untreated controls or cells exposed to PHF alone (ratio pSer199/NeuN 4.26, 4.57, and 4.50, $p = 0.0005$, 0.0001, and 0.0006 relative to untreated samples, $p = 0.047$, 0.013, and 0.040 relative to PHF alone, overall $p < 0.0001$, one-way ANOVA).

Bars represent average ± SEM.

$p \leq 0.05$, ## $p \leq 0.01$, ### $p \leq 0.001$, #### $p < 0.0001$, * $p \leq 0.05$, ** $p \leq 0.01$, *** $p \leq 0.001$, **** $p < 0.0001$.

significant compared to untreated control, * significant compared to PHF alone.

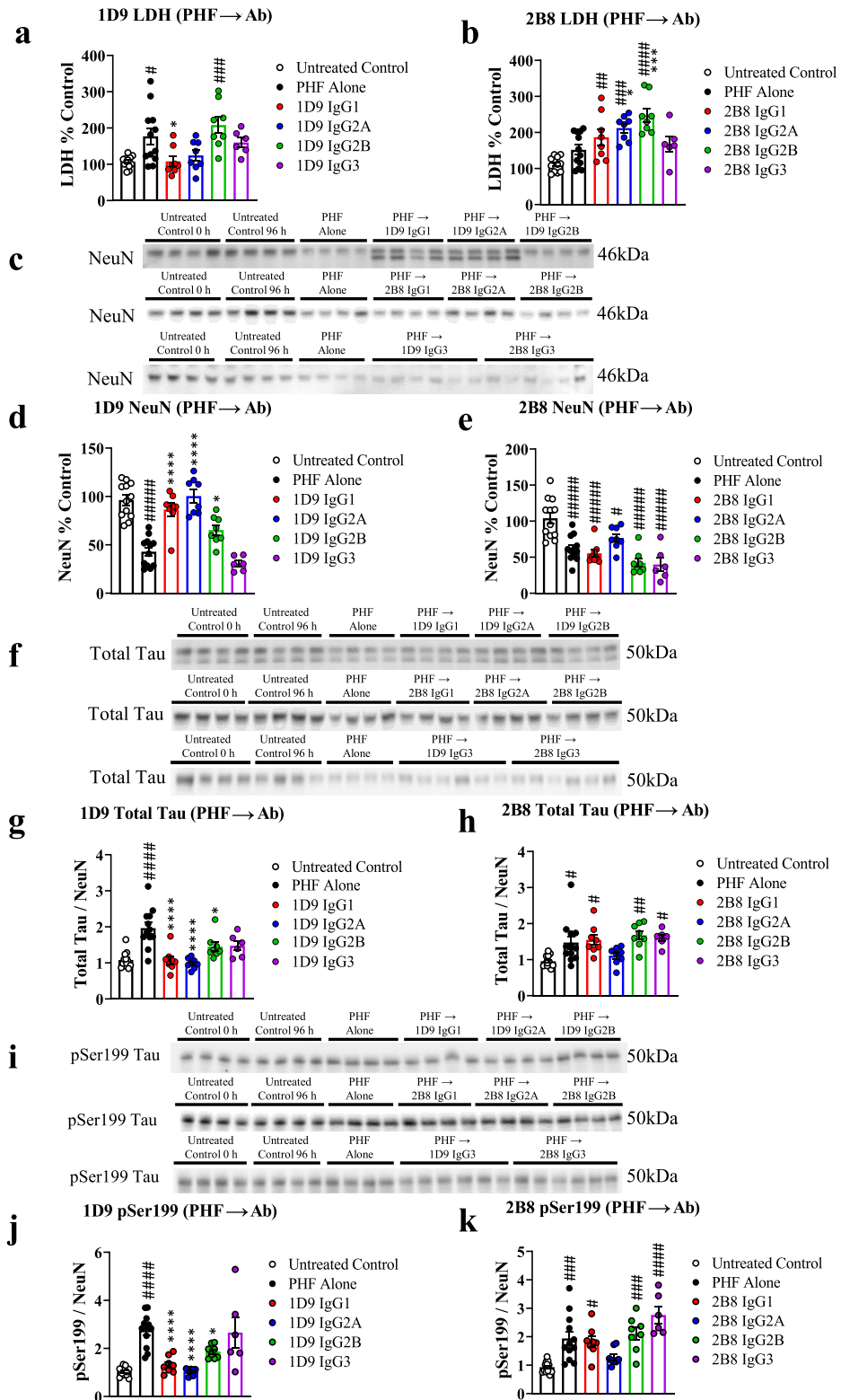


Figure 7. In the PHF → Ab dosing paradigm, 1D9 IgG1 and IgG2A are the most efficacious subclasses in preventing PHF-induced toxicity and seeding. All 2B8 IgG subclasses are toxic. Mixed JNPL3 cultures were incubated with 10 μg/ml PHF followed 24 h later by 10 μg/ml IgG subclasses (n = at least 6 replicates per condition). Cells were collected 96 h after the antibody

colocalized with neurons (IgG1 75%, IgG2A 62%, IgG2B 65%, and IgG3 71%, Figure 8d) with no significant differences in colocalization between groups. Thus, while IgG3 had an overall lower level of uptake, its internalization was mainly neuronal. Similar overall uptake results were seen using the four 2B8 subclasses. 2B8 IgG1, IgG2A and IgG2B were taken up into cells to a similar extent with IgG3 significantly less so after an hour of incubation (overall p value < 0.0001 , $p = 0.0002$, 0.0007 , 0.0002 relative to IgG1, IgG2A and IgG2B, one-way ANOVA, Supplemental Figure 4).

In a second set of experiments, we incubated mixed neuron/glia cultures with each antibody subclass and $1 \mu\text{g/ml}$ PHF. We have previously shown that adding PHF and antibody together to cultures results in complexes of the two,³³ and other groups have shown that antibody bound tau can be cleared via microglia in an Fc-dependent manner.^{19,20,31,54–57} Because phagocytosis of exogenous tau requires Fc receptor binding, it is also likely to be impacted by subclass.

To test the ability of 1D9 subclasses to promote microglial phagocytosis of extracellular exogenous PHF tau, microglia were labeled in the live cultures using tomato lectin (Figure 8e). In the presence of human derived PHF-tau, 1D9 IgG3 again had significantly lower cellular uptake compared with IgG1 and IgG2B, with a trend towards lower uptake compared to IgG2A ($p = 0.001$, $= 0.002$, $= 0.08$, respectively, overall $p = 0.0002$, one-way ANOVA, Figure 8f). In the presence of exogenous tau, cellular uptake also shifted from neurons to microglia, with the majority of the IgG1, IgG2A and IgG2B signal colocalizing with the microglia (IgG1 82%, IgG2A 77%, IgG2B 82%, Figure 8g). In

contrast, and analogous to the neuronal uptake, IgG3 was significantly less in microglia compared to the other subclasses (46% colocalization, $p = 0.0015$, $= 0.008$, $= 0.001$, compared to IgG1, IgG2A, and IgG2B, respectively, overall $p = 0.0003$, one-way ANOVA, Figure 8g).

In summary, the uptake study provides an additional explanation for 1D9 IgG3's lack of efficacy. Its uptake into neurons is reduced which would render the antibody less able to bind to and clear pathological tau that has already been internalized in the PHF \rightarrow Ab paradigm. It is also less capable of promoting microglial phagocytosis of extracellular tau in the PHF + Ab dosing condition, which fits with known features of the mouse IgG3 subtype. It is relatively neutral with regard to effector function, such as microglial phagocytosis, comparable to human IgG4.^{58–64}

1D9 IgG1 and IgG2A show improved clearance of tau within the brain interstitial fluid relative to their sdAb in vivo

We then tested 1D9 and 2B8 IgG1 and IgG2A, along with their respective sdAbs, for efficacy in clearing tau from brain interstitial fluid (ISF) in vivo. JNPL3 females 7–11 months old were fitted with the probe and fluid was collected for 8 h prior to antibody infusion to establish a baseline level. This baseline collection occurred during the animals' inactive period when ISF tau levels are at their lowest. The concentration of tau in the ISF fluctuates during a 24 h period with levels peaking during the night when the animals are most active.⁶⁵ Samples were collected from control and antibody treated animals for a total of 32 h, the 8 h baseline plus 24 h post-

application. **a.** In the 1D9 group, PHF alone increased LDH levels and 1D9 IgG2B had no effect on PHF toxicity (177 and 208 % of control values, $p = 0.02$ and 0.0008 , overall $p = 0.0002$, one-way ANOVA). In contrast, 1D9 IgG1 prevented PHF toxicity (108% of control, $p = 0.05$). **b.** In the 2B8 group, there was an overall treatment effect ($p < 0.0001$, one-way ANOVA). 2B8 IgG1, IgG2A and IgG2B samples had increased LDH relative to untreated samples (187, 214, and 248% of control values, $p = 0.009$, $= 0.0002$, and < 0.0001), and IgG2A and IgG2B treated cells were also elevated compared to PHF alone ($p = 0.05$, 0.0004). **c.** Immunoblots showing NeuN levels in the control and treated JNPL3 cultures. **d.** In the 1D9 group, PHF alone decreased NeuN (43% of control, $p < 0.0001$, overall $p < 0.0001$, one-way ANOVA). 1D9 IgG1, IgG2A, and IgG2B prevented this toxicity (NeuN levels 86, 100, and 65% of control values, $p < 0.0001$, < 0.0001 , and 0.04 respectively). **e.** In the 2B8 group, PHF alone was toxic as measured by NeuN levels (62% of control, $p < 0.0001$, overall $p < 0.0001$, one-way ANOVA). None of the 2B8 IgG subtypes prevented the PHF-induced toxicity and had reduced NeuN levels relative to untreated control cells (55, 77, 42, and 34% of control values, $P < 0.0001$, 0.04 , < 0.0001 , < 0.0001). **f.** Immunoblots from the same JNPL3 cell lysate used in the toxicity experiments were probed for total tau. **g.** In the 1D9 group, PHF alone increased intracellular tau relative to untreated control (ratio tau/NeuN 1.96, $p < 0.0001$, overall $p < 0.0001$, one-way ANOVA). 1D9 IgG1, IgG2A and IgG2B prevented tau seeding (ratio tau/NeuN 1.05, 0.97, 1.39, $p < 0.0001$ compared to PHF alone for all). **h.** In the 2B8 group, PHF alone increased total tau in the cells (ratio tau/NeuN 1.47, $p = 0.016$, overall $p = 0.0003$, one-way ANOVA). Cells treated with 2B8 IgG1, IgG2B and IgG3 also had higher total tau relative to untreated control (ratio tau/NeuN 1.55, 1.68 and 1.61, $p = 0.013$, 0.0015 , and 0.013), and none of the antibodies prevented the PHF-induced tau seeding. **i.** The same samples were used in immunoblotting to measure tau phosphorylated at Ser199. **j.** In the 1D9 group, PHF increased intracellular phospho-tau (pSer199/NeuN ratio 2.76, $p < 0.0001$, overall $p < 0.0001$, one-way ANOVA). 1D9 IgG1, IgG2A and IgG2B prevented this increase (ratio pSer199/NeuN 1.31, 1.03, and 1.86, $p < 0.0001$, < 0.0001 , 0.03). **k.** In the 2B8 group, PHF alone increased phospho-tau seeding (ratio pSer199/NeuN 1.93, $p = 0.001$, overall $p < 0.0001$, one-way ANOVA). Cells treated with 2B8 IgG1, IgG2A and IgG3 also had an increase in pSer199 relative to the untreated controls (ratio pSer199/NeuN 1.83, 2.11, 2.76, $p = 0.013$, 0.0005 , < 0.0001), with none of the subtypes resulting in different pSer199 levels relative to PHF alone.

Bars represent average \pm SEM.

$p \leq 0.05$, ## $p \leq 0.001$, ### $p \leq 0.001$, #### $p < 0.0001$, * $p \leq 0.05$, ** $p \leq 0.01$, *** $p \leq 0.001$, **** $p < 0.0001$.

significant compared to untreated control, * significant compared to PHF alone.

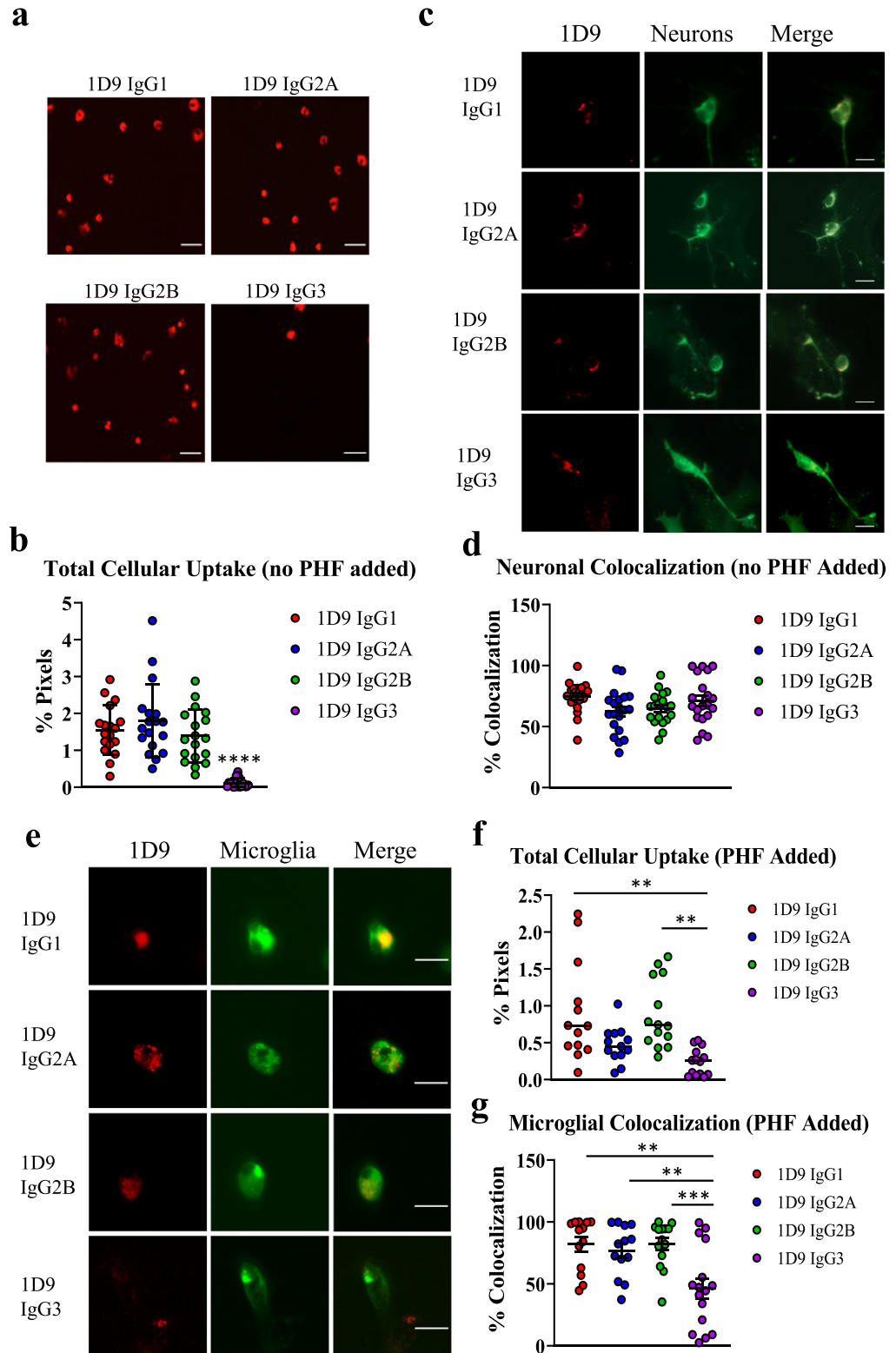


Figure 8. 1D9 IgG3 has lower neuronal and microglial uptake relative to other IgG subclasses. Each 1D9 IgG subtype was labeled with CypHer5, a pH sensitive dye that fluoresces in acidic compartments such as the endosomal/lysosomal system. **a.** Mixed cortical JNPL3 cultures were incubated with 5 μ g/ml of the labeled antibodies for one h without addition of exogenous PHF, after

infusion, and their tau levels in ISF were assessed by ELISA.

In control animals, the normal diurnal pattern was observed with tau levels peaking 9–10 h following the collection of baseline samples. A two-way ANOVA for the 1D9 treated animals showed significant antibody, time, and interaction effects ($p < 0.0001$, $= 0.0088$ and < 0.0001 , respectively). Animals infused with a 50 $\mu\text{g}/\text{ml}$ solution of 1D9 sAb for two h (total of 7.2 μg injected), showed a somewhat muted diurnal increase with ISF tau levels significantly lower compared to controls at 7–10 h post-infusion ($p = 0.027$ and 0.0055 for 7–8 h and 9–10 h, [Figure 9a](#)). In mice receiving an equimolar concentration of 1D9 IgG1 or IgG2A, this effect was even greater. Both antibodies strongly reduced ISF tau levels below control values. 1D9 IgG1 infused animals had significantly lower ISF tau levels than untreated controls from 3 h through 18 h ($p = 0.033$ to $p < 0.0001$, [Figure 9a](#)). Likewise, 1D9 IgG2A infused animals had significantly lower ISF tau levels than controls from immediately post-infusion to 18 h ($p = 0.045$ to $p < 0.0001$, [Figure 9a](#)). 1D9 IgG1 values were significantly lower than its respective sAb as well at 5–6 h and 9–10 h ($p = 0.035$ and 0.025 , [Figure 9a](#)). This can also be seen when the post-infusion samples were pooled. Animals treated with 1D9 sAb, IgG1 and IgG2A all showed significantly lower ISF tau levels after antibody infusion ($p < 0.0001$ for all, overall $p < 0.0001$, [Figure 9b](#)). The whole 1D9 IgG1 and IgG2A were also significantly more efficacious than the sAb ($p < 0.0001$ for both, [Figure 9b](#)).

In contrast, 2B8 IgG1 and IgG2A performed significantly less well than their sAb. As with 1D9, a total of 7.2 μg of the 2B8 sAb was injected over two h, or the molar equivalent of IgG1 or IgG2A. There were significant overall antibody, time and interaction effects using a two-way ANOVA ($p < 0.0001$, $= 0.0033$, < 0.0001 , two-way ANOVA). The 2B8 sAb samples had significantly lower tau from the first post-infusion time point through 22 h ($p = 0.011$ to $p < 0.0001$, [Figure 9c](#)). 2B8 IgG1 did prevent the activity-based tau increase, but the effect was not as strong as that seen with the 2B8 sAb,

only lasting between 3–14 h ($p = 0.035$ to $p < 0.0001$, one-way ANOVA, [Figure 9c](#)). With 2B8 IgG2A the effect was also shorter lived, with efficacy only at 5–8 h ($p = 0.029$ and 0.0001 at 5–6 h and 7–8 h, [Figure 9c](#)). 2B8 sAb tau values were significantly lower than 2B8 IgG1 at 11–12 h and 15–20 h ($p = 0.048$ to $p = 0.0055$, [Figure 9c](#)). This was even more pronounced with IgG2A which resulted in significantly higher ISF tau levels than the sAb from 9–20 h ($p = 0.035$ to $p < 0.0001$, [Figure 9c](#)). With the pooled samples, 2B8 sAb, IgG1, and IgG2A all lowered ISF tau levels, compared to controls ($p < 0.0001$, $p < 0.0001$ and $p = 0.0003$, respectively, overall $p < 0.0001$, one-way ANOVA, [Figure 9d](#)). However, the 2B8 IgG1 and IgG2A treatment groups had significantly higher pooled ISF tau levels post-infusion, compared to their sAb ($p = 0.004$, < 0.0001 for IgG1 and IgG2A, [Figure 9d](#)).

Together, these in vivo findings on the efficacy of the two unmodified univalent sAbs and the two most effective subtypes indicate that addition of the IgG scaffold increases 1D9's efficacy relative to its sAb, potentially through enhancement of microglial phagocytosis via Fc receptors. However, for 2B8, the addition of a second tau binding site compromises its activity and leads to toxicity, as per the culture data, possibly by stabilizing a toxic conformation of tau.

Discussion

Herein we demonstrate that despite retaining identical variable regions, adding constant domains, or swapping between IgG subclasses can result in antibodies with very different efficacy/safety profiles. We selected two camelid single domain antibodies, 1D9 and 2B8, from a screening of clones isolated from a llama immunized with a recombinant (rec) human tau protein and paired helical filament (PHF)-enriched tau isolated from a human tauopathy brain. Initial testing in primary mouse neurons showed that the two were not toxic, were taken up into neurons to a similar degree, and prevented the toxicity and tau seeding induced by

which live images were collected from each well (scale = 30 μm). **b.** The total number of pixels in each image ($n = 18$ images per group) that contained the antibody signal was determined, and 1D9 IgG3 showed significantly lower uptake compared to all three other subtypes ($p < 0.0001$ for all, overall $p < 0.0001$, one-way ANOVA). **c.** An additional group of cells was fixed and then stained with a total tau antibody to visualize neurons (scale = 20 μm). **d.** All 1D9 IgG subtypes showed a similar high degree of colocalization between the antibody and neurons (IgG1 75%, IgG2A 62%, IgG2B 65%, and IgG3 71%, $n = 20$ images per group), indicating that in the absence of exogenous tau, most antibody uptake is neuronal. **e.** CypHer 5 labeled 1D9 IgG subtypes (5 $\mu\text{g}/\text{ml}$) and human derived PHF-tau (1 $\mu\text{g}/\text{ml}$) were added to mixed neuron/glia cultures at the same time. Cultures were also incubated with fluorescent tomato lectin to label microglia. Live cell images of the cultures showed a high degree of antibody colocalization with glia for 1D9 IgG1, IgG2A and IgG2B after one h incubation (scale = 20 μm). **f.** Overall uptake in each image ($n = 15$ images per group) was determined, and 1D9 IgG3 had less uptake than either IgG1 or IgG2B ($p = 0.001$ and 0.002 , overall $p = 0.0002$, one-way ANOVA). **g.** 1D9 IgG1, IgG2A and IgG2B showed a shift to a majority microglial uptake in the presence of PHF (82, 77, and 82%). IgG3 in contrast did not and its percentage of microglial uptake was lower relative to the other three (46% colocalization, $p = 0.0015$, 0.008 , and 0.001 for IgG1, IgG2A, and IgG2B, overall $p = 0.0003$, one-way ANOVA).

Bars represent average \pm SEM.

** $p \leq 0.05$, *** $p \leq 0.001$, **** $p < 0.0001$.

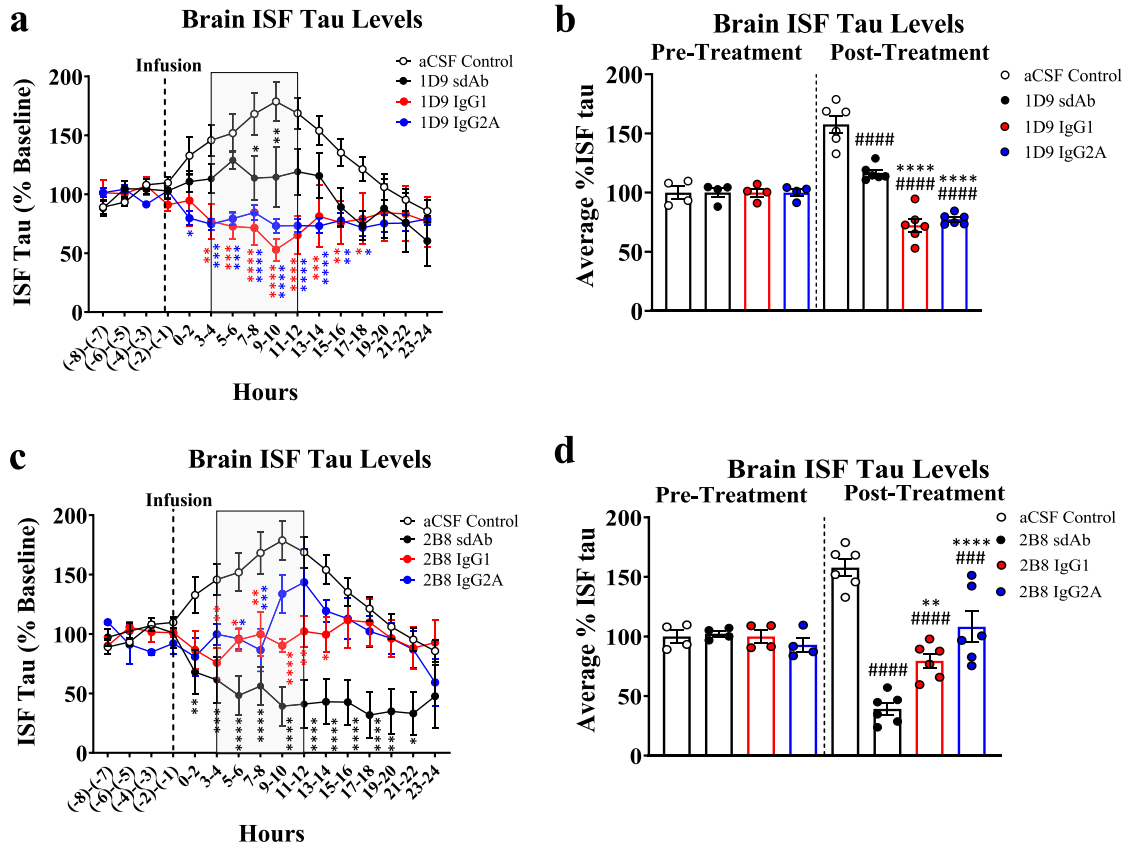


Figure 9. 1D9 IgG1 and IgG2A improve clearance of interstitial tau relative to their sdAb *in vivo*, whereas the 2B8 IgG subclasses are less effective than their sdAb. Brain interstitial fluid (ISF) was collected from JNPL3 mice aged 7–11 months infused with 1D9 or 2B8 sdAb (n = 6 per group), whole IgG1 or IgG2A (n = 6 per group), or artificial CSF (aCSF) vehicle (n = 11). Baseline samples were collected during the animals’ inactive period, and then for a further 24 hours following antibody administration. The shaded boxes in panels A and C represent the typical dark (awake) cycle for the mice. Even though the animals were maintained in constant light, they display the typical diurnal pattern of tau release during the first 24 h. **a.** In mice receiving 1D9, there were significant antibody, time, and interaction effects (p < 0.0001, = 0.0088, < 0.0001 respectively, two-way ANOVA). 1D9 sdAb treated animals had lower ISF tau levels relative to untreated controls at 7–10 h post-infusion (p = 0.027 and 0.0055 for 7–8 h and 9–10 h). 1D9 IgG1 infused animals were lower than untreated mice from 3–18 h (p values range from 0.033 through < 0.0001), and IgG2A treated mice from 0–18 h (p values range from 0.045 through < 0.0001). 1D9 IgG1 samples were lower than their sdAb at 5–6 h and 9–10 h (p = 0.035 and 0.025). **b.** When post-infusion samples were pooled, 1D9 sdAb, IgG1 and IgG2A samples were all lower than untreated control samples (p < 0.0001 for all, overall p < 0.0001, one-way ANOVA). IgG1 and IgG2A were also more effective at preventing the activity related tau increase compared to the sdAb (p < 0.0001 for both). **c.** In mice receiving 2B8, there were significant treatment, time, and interaction effects (p < 0.0001, = 0.0033, < 0.0001, two-way ANOVA). 2B8 sdAb treated mice had lower ISF tau compared to untreated animals from 0–22 h (p values range from 0.011 through < 0.0001). 2B8 IgG1 treated mice had lower tau levels at 3–14 h (p values range from 0.035 through < 0.0001), and 2B8 IgG2A treated mice only at 5–8 h (p = 0.029 and 0.0001 at 5–6 h and 7–8 h). 2B8 IgG1 values were also higher than its sdAb at 11–12 h and 15–20 h (p values range from 0.048 through 0.0055), and 2B8 IgG2A values were higher at 9–20 h (p values range from 0.035 through < 0.0001). **d.** All pooled 2B8 sdAb samples had lower ISF tau than untreated controls (p < 0.0001, < 0.0001, = 0.0003, overall p < 0.0001, one-way ANOVA). Post infusion samples from mice treated with 2B8 IgG1 and IgG2A had higher tau levels compared to their sdAb (p = 0.004 and < 0.0001). Points and bars represent average ± SEM.

p < 0.0001, * p ≤ 0.05, ** p ≤ 0.01, *** p ≤ 0.001, **** p < 0.0001.

Panels a and c: * sdAb relative to untreated, * IgG1 relative to untreated, * IgG2A relative to untreated controls.

Panels b and d: # significant compared to untreated control, * significant compared to sdAb.

exposure to pathological tau. The 2B8 sdAb was the more efficacious of the two, as it showed significant benefits in both toxicity assays, LDH and NeuN immunoblotting. These positive findings supported

further testing and thus, the sdAbs served as the basis for generating an array of subclass variants.

Because antibody subclass potentially impacts both neuronal and glial mechanisms, the variants were

assessed first in mixed cortical cultures, which contain all cell types. Interestingly, while both 1D9 and 2B8 were non-toxic as unmodified sdAbs and prevented PHF-induced toxicity in neuronal culture (Supplemental Figure 1 and Figure 2), their IgG subclasses had a different toxicity profile (Figures 5-7). The Fc(sdAb)₂ subclasses of 2B8 were toxic in otherwise untreated mixed JNPL3 tauopathy neuron/glia culture, whereas the 1D9 subclasses were not. In cultures exposed to PHF, the four 1D9 IgG subclasses containing the same tau binding region, clearly differed in efficacy in both intra- and extracellular dosing paradigms. IgG1 and IgG2A subclasses prevented PHF-induced loss of NeuN in both the PHF + Ab (extracellular) and PHF → Ab (intracellular) dosing methods. The IgG2B subclass of 1D9 showed some efficacy in preventing toxicity as measured by NeuN levels in the intracellular paradigm, but not in other measures. The IgG3 subclass of 1D9 was ineffective in both conditions on all measures. In contrast to 1D9, all of the 2B8 subclasses were toxic in the primary tauopathy cultures, and some of them even enhanced PHF-induced toxicity. Using NeuN analysis of cell lysates as an indicator of toxicity seemed to be more sensitive than LDH measurement of media. This is in line with our prior studies in this culture model,^{32,33} and can be explained by the fact that NeuN levels are decreased both by loss of neurons and retraction of cellular processes, whereas LDH increase reflects only cell death.

Differences between antibodies and subclasses were likewise obtained when measuring tau seeding activity. 1D9 IgG1 and IgG2A prevented the PHF-induced increases in total and phosphorylated intracellular tau levels in both the PHF + Ab and PHF → Ab paradigms, thus showing efficacy in targeting both intra- and extracellular tau. 1D9 IgG2B again showed efficacy only in the intracellular paradigm, and IgG3 not at all. As in the toxicity experiments, the 2B8 subclasses did not prevent tau seeding and in some cases promoted it.

Together these data showed a consistent pattern where 1D9 IgG1 and IgG2A were the most efficacious in both dosing paradigms, with IgG2B showing some efficacy in the PHF → Ab condition. As stated above, we have shown that multiple factors influence efficacy, and despite sharing an identical variable region, 1D9 IgG2B and IgG3 do not have the same ability as the other two subclasses to prevent PHF-induced pathology.

These differences between the sdAbs and their Fc-(sdAb)₂ subclasses in the culture models were also reflected in the *in vivo* microdialysis target engagement study. Specifically, the 1D9 IgG1 and IgG2A subclasses showed improved *in vivo* efficacy in clearing tau, relative to their sdAb, whereas these two 2B8 subclasses were less effective than their sdAb counterpart.

The ineffectiveness of 1D9 IgG3 is the simplest of these to explain. Firstly, it was the only subclass to not

show reduced binding to the plate in the competitive ELISA. Our published results show that antibodies that are more efficacious, preferentially bind to soluble rather than plate bound tau.^{32,33} We have further shown that uptake into neurons is required for clearance of intracellular pathological tau, and that uptake of whole Fc-antibodies into neurons is largely mediated by low affinity FcγII/III receptors.^{33,66} Similarly, blocking Fc receptors or using effectorless antibodies inhibits microglial removal of tau from the extracellular space.¹⁹ Total cellular uptake of the IgG3 subclass of 1D9 was significantly lower in the mixed culture than for the three other subclasses both alone and in the presence of PHF-enriched tau. This limited uptake, and impaired ability to promote microglial phagocytosis thus contributes to its ineffectiveness. Its lack of effector function is considered to be equivalent to human IgG4. Compared to other subclasses, mouse IgG3 shows minimal to no binding to murine FcγII, III, and IV receptors and its binding to FcγI receptors has not been shown consistently.⁵⁸⁻⁶⁴ Thus, its uptake is too limited to neutralize or clear pathological tau, either directly in neurons or via microglial phagocytosis.

The likely reason for the relative ineffectiveness of 1D9 IgG2B is not as straightforward. It has a similar uptake profile as its IgG1 and IgG2A counterparts, so that is not the reason for its limited efficacy. However, ELISA assays showed that it had substantially higher affinity for solid-phase PHF-tau over the other two subclasses. Such high binding has in past experiments with other traditional mouse monoclonal tau antibodies been associated with less efficacy, presumably because less of it is then available to bind to more toxic soluble tau.^{32,33} The question then arises as to why antibodies with the same tau binding variable region would have different affinities. We have previously observed this phenomenon when creating a partially humanized tau antibody chimera, suggesting that non-binding regions of antibodies influence their binding, presumably by altering their flexibility and/or conformation.³² While this topic has not been thoroughly studied in tau antibodies, researchers in other fields have shown that changing constant domains of IgG can alter binding even when the variable region remains the same.⁶⁷⁻⁸² Collectively, these findings then clarify why the IgG2B subtype of 1D9 has a different binding profile compared to the other subtypes, which may explain its lack of efficacy despite favorable neuronal and glial uptake.

Regarding the toxic effects of the 2B8 Fc-(sdAb)₂ subclasses compared to the beneficial effects of the 2B8 sdAb, it may relate to stabilization of a toxic conformation of tau that requires the two arms of the sdAb acting in concert. The lack of toxicity in the wild-type mouse cells supports this idea. In addition, as detailed above, the constant domain may lead to structural changes that may affect its binding profile and thereby toxicity. In the solution phase binding assays, avidity of the 2B8

Fc(sdAb)₂ is increased for all of the tau forms tested relative to the 2B8 sdAb, as expected when a second binding site is added.

These data emphasize the importance of subclasses to antibody efficacy and toxicity and highlight that the antigen and Fc binding portions of the molecule are not independent entities. For 1D9, although being generated from the same sdAb, the IgG subtypes have different uptake, efficacy, and binding profiles, and are more effective in clearing tau in vivo than the unmodified sdAb. In contrast, while the 2B8 sdAb was safe and efficacious, its subclasses became toxic and less effective in vivo. These findings have major implications for clinical development of therapeutic antibodies targeting the tau protein or other targets.

Contributors

Conceptualization: E.E.C., E.M.S.; Formal Analysis: E.E.C., L.A.S-B, A.D.; Investigation: E.E.C., A.D., L.A.S-B., Y. J.; Verification of underlying data: E.E.C., A.D., L.A.S-B., Y.J., E.M.S.; Resources: R.P., Y.L., M.L., M.H.K., X.P.K.; Data Curation: E.E.C., E.M.S.; Writing-Original Draft: E. E.C.; Writing-Review & Editing: E.E.C., L.A.S-B., E.M. S., X.P.K.; Visualization: E.E.C., E.M.S.; Supervision: E. E.C., X.P.K., E.M.S.; Project Administration: E.M.S.; Funding Acquisition: E.M.S., X.P.K. All authors read and approved the final version of the manuscript. EMS and each author responsible for the individual analyses verified the underlying data.

Data sharing statement

Research data that documents, supports, and validates research findings is available via a reasonable request to the corresponding author. Data will also be presented at national meetings.

Declaration of interests

EMS is an inventor on patents on tau immunotherapies and related diagnostics, which are assigned to New York University, and some of those are licensed to H. Lundbeck A/S. Notably, this licensing does not include tau sdAbs such as the 2B8 and 1D9 antibodies used in these experiments. All other authors have nothing to declare.

Acknowledgements

EMS is supported by NIH grants [R01 AG032611](#), [R01 NS077239](#), [RF1 NS120488](#) and [R21 AG 069475](#). This work was also supported by [R21 AG 058282](#) (EMS), NYU Alzheimer's Disease Center NIH Pilot Grant (via [P30 AG008051](#); LASB), and [T32AG052909](#) (AD). We thank the team at Prosci Inc for their contracted work, in particular Andy Lee.

Supplementary materials

Supplementary material associated with this article can be found in the online version at [doi:10.1016/j.ebiom.2022.104249](https://doi.org/10.1016/j.ebiom.2022.104249).

References

- Ji C, Sigurdsson EM. Current status of clinical trials on tau immunotherapies. *Drugs*. 2021;81(10):1135–1152.
- Sandusky-Beltran LA, Sigurdsson EM. Tau immunotherapies: lessons learned, current status and future considerations. *Neuropharmacology*. 2020;175:108104.
- Congdon EE, Jiang Y, Sigurdsson EM. Targeting tau only extracellularly is likely to be less efficacious than targeting it both intra- and extracellularly. *Semin Cell Dev Biol*. 2022;126:125–137.
- Bittar A, Bhatt N, Kaye R. Advances and considerations in AD tau-targeted immunotherapy. *Neurobiol Dis*. 2020;134:104707.
- Plotkin SS, Cashman NR. Passive immunotherapies targeting Aβ and tau in Alzheimer's disease. *Neurobiol Dis*. 2020;144:105010.
- Colin M, Dujardin S, Schraen-Maschke S, et al. From the prion-like propagation hypothesis to therapeutic strategies of anti-tau immunotherapy. *Acta Neuropathol*. 2020;139(1):3–25.
- Sigurdsson EM. Alzheimer's therapy development: a few points to consider. *Prog Mol Biol Transl Sci*. 2019;168:205–217.
- Han P, Serrano G, Beach TG, et al. A quantitative analysis of brain soluble tau and the tau secretion factor. *J Neuropathol Exp Neurol*. 2017;76(1):44–51.
- Barthelemy NR, Gabelle A, Hirtz C, et al. Differential mass spectrometry profiles of tau protein in the cerebrospinal fluid of patients with Alzheimer's disease, progressive supranuclear palsy, and dementia with lewy bodies. *J Alzheimers Dis*. 2016;51(4):1033–1043.
- Barthelemy NR, Fenaille F, Hirtz C, et al. Tau protein quantification in human cerebrospinal fluid by targeted mass spectrometry at high sequence coverage provides insights into its primary structure heterogeneity. *J Proteome Res*. 2016;15(2):667–676.
- Sato C, Barthelemy NR, Mawuenyega KG, et al. Tau kinetics in neurons and the human central nervous system. *Neuron*. 2018;97(6):1284–1298.e7.
- Wagshal D, Sankaranarayanan S, Guss V, et al. Divergent CSF tau alterations in two common tauopathies: Alzheimer's disease and progressive supranuclear palsy. *J Neurol Neurosurg Psychiatry*. 2015;86(3):244–250.
- Hall S, Ohrfelt A, Constantinescu R, et al. Accuracy of a panel of 5 cerebrospinal fluid biomarkers in the differential diagnosis of patients with dementia and/or parkinsonian disorders. *Arch Neurol*. 2012;69(11):1445–1452.
- Hu WT, Trojanowski JQ, Shaw LM. Biomarkers in frontotemporal lobar degenerations—progress and challenges. *Prog Neurobiol*. 2011;95(4):636–648.
- Olsson B, Lautner R, Andreasson U, et al. CSF and blood biomarkers for the diagnosis of Alzheimer's disease: a systematic review and meta-analysis. *Lancet Neurol*. 2016;15(7):673–684.
- Bian H, Van Swieten JC, Leight S, et al. CSF biomarkers in frontotemporal lobar degeneration with known pathology. *Neurology*. 2008;70(19 Pt 2):1827–1835.
- Grossman M, Farmer J, Leight S, et al. Cerebrospinal fluid profile in frontotemporal dementia and Alzheimer's disease. *Ann Neurol*. 2005;57(5):721–729.
- Lee SH, Le Pichon CE, Adolphsson O, et al. Antibody-mediated targeting of tau in vivo does not require effector function and microglial engagement. *Cell Rep*. 2016;16(6):1690–1700.
- Zilkova M, Nolle A, Kovacech B, et al. Humanized tau antibodies promote tau uptake by human microglia without any increase of inflammation. *Acta Neuropathol Commun*. 2020;8(1):74.
- Andersson CR, Falsig J, Stavenhagen JB, et al. Antibody-mediated clearance of tau in primary mouse microglial cultures requires Fcγ-receptor binding and functional lysosomes. *Sci Rep*. 2019;9(1):4658.
- Asai H, Ikezu S, Tsunoda S, et al. Depletion of microglia and inhibition of exosome synthesis halt tau propagation. *Nat Neurosci*. 2015;18(11):1584–1593.
- Shi Y, Manis M, Long J, et al. Microglia drive APOE-dependent neurodegeneration in a tauopathy mouse model. *J Exp Med*. 2019;216(11):2546–2561.
- Mancuso R, Fryatt G, Cleal M, et al. CSF1R inhibitor JNJ-40346527 attenuates microglial proliferation and neurodegeneration in P301S mice. *Brain*. 2019;142(10):3243–3264.
- Gratze M, Chen Y, Parhizkar S, et al. Activated microglia mitigate Aβ-associated tau seeding and spreading. *J Exp Med*. 2021;218(8):e20210542.

- 25 Hassan-Abdi R, Brenet A, Bennis M, Yanicostas C, Soussi-Yanicostas N. Neurons expressing pathological tau protein trigger dramatic changes in microglial morphology and dynamics. *Front Neurosci*. 2019;13:1199.
- 26 Clayton K, Delpach JC, Herron S, et al. Plaque associated microglia hyper-secrete extracellular vesicles and accelerate tau propagation in a humanized APP mouse model. *Mol Neurodegener*. 2021;16(1):18.
- 27 Wang C, Fan L, Khawaja RR, et al. Microglial NF-kappaB drives tau spreading and toxicity in a mouse model of tauopathy. *Nat Commun*. 2022;13(1):1969.
- 28 Brelstaff JH, Mason M, Katsinelos T, et al. Microglia become hypofunctional and release metalloproteases and tau seeds when phagocytosing live neurons with P301S tau aggregates. *Sci Adv*. 2021;7(43):eabg4980.
- 29 Hopp SC, Lin Y, Oakley D, et al. The role of microglia in processing and spreading of bioactive tau seeds in Alzheimer's disease. *J Neuroinflamm*. 2018;15(1):269.
- 30 Ayalon G, Lee SH, Adolfsson O, et al. Antibody semorinemab reduces tau pathology in a transgenic mouse model and engages tau in patients with Alzheimer's disease. *Sci Transl Med*. 2021;13(593):eabb2639.
- 31 Bajracharya R, Brici D, Bodea LG, Janowicz PW, Gotz J, Nisbet RM. Tau antibody isotype induces differential effects following passive immunisation of tau transgenic mice. *Acta Neuropathol Commun*. 2021;9(1):42.
- 32 Congdon EE, Chukwu JE, Shamir DB, et al. Tau antibody chimerization alters its charge and binding, thereby reduces its cellular uptake and efficacy. *eBioMedicine*. 2019;42:157-173.
- 33 Congdon EE, Lin Y, Rajamohamedsait HB, et al. Affinity of tau antibodies for solubilized pathological tau species but not their immunogen or insoluble tau aggregates predicts in vivo and ex vivo efficacy. *Mol Neurodegener*. 2016;11(1):62-86.
- 34 Liu M, Sui D, Dexheimer T, et al. Hyperphosphorylation renders tau prone to aggregate and to cause cell death. *Mol Neurobiol*. 2020;57(11):4704-4719.
- 35 Sui D, Xu X, Ye X, et al. Protein interaction module-assisted function X (PIMAX) approach to producing challenging proteins including hyperphosphorylated tau and active CDK5/p25 kinase complex. *Mol Cell Proteomics*. 2015;14(1):251-262.
- 36 Lewis J, McGowan E, Rockwood J, et al. Neurofibrillary tangles, amyotrophy and progressive motor disturbance in mice expressing mutant (P301L) tau protein. *Nat Gen*. 2000;25(4):402-405.
- 37 Murphy KE, Gysbers AM, Abbott SK, et al. Reduced glucocerebrosidase is associated with increased alpha-synuclein in sporadic Parkinson's disease. *Brain*. 2014;137(Pt 3):834-848.
- 38 Park S, Jung Y. Combined actions of Na/K-ATPase, NCX1 and glutamate dependent NMDA receptors in ischemic rat brain penumbra. *Anat Cell Biol*. 2010;43(3):201-210.
- 39 McKiernan RC, Jimenez-Mateos EM, Bray I, et al. Reduced mature microRNA levels in association with dicer loss in human temporal lobe epilepsy with hippocampal sclerosis. *PLoS One*. 2012;7(5):e35921.
- 40 Karuppagounder SS, Shi Q, Xu H, Gibson GE. Changes in inflammatory processes associated with selective vulnerability following mild impairment of oxidative metabolism. *Neurobiol Dis*. 2007;26(2):353-362.
- 41 Jin N, Yin X, Yu D, et al. Truncation and activation of GSK-3beta by calpain I: a molecular mechanism links to tau hyperphosphorylation in Alzheimer's disease. *Sci Rep*. 2015;5:8187.
- 42 Larson M, Sherman MA, Amar F, et al. The complex PrP(c)-Fyn couples human oligomeric Abeta with pathological tau changes in Alzheimer's disease. *J Neurosci*. 2012;32(47):16857-71a.
- 43 Morozova V, Cohen LS, Makki AE, et al. Normal and pathological tau uptake mediated by M1/M3 muscarinic receptors promotes opposite neuronal changes. *Front Cell Neurosci*. 2019;13:403.
- 44 Yoshiyama Y, Zhang B, Bruce J, Trojanowski JQ, Lee VM. Reduction of detyrosinated microtubules and Golgi fragmentation are linked to tau-induced degeneration in astrocytes. *J Neurosci*. 2003;23(33):10662-10671.
- 45 Fulga TA, Elson-Schwab I, Khurana V, et al. Abnormal bundling and accumulation of F-actin mediates tau-induced neuronal degeneration in vivo. *Nat Cell Biol*. 2007;9(2):139-148.
- 46 Cowan CM, Bossing T, Page A, Shepherd D, Mudher A. Soluble hyper-phosphorylated tau causes microtubule breakdown and functionally compromises normal tau in vivo. *Acta Neuropathol*. 2010;120(5):593-604.
- 47 Li B, Chohan MO, Grundke-Iqbal I, Iqbal K. Disruption of microtubule network by Alzheimer abnormally hyperphosphorylated tau. *Acta Neuropathol*. 2007;113(5):501-511.
- 48 Rane JS, Kumari A, Panda D. An acetylation mimicking mutation, K274Q, in tau imparts neurotoxicity by enhancing tau aggregation and inhibiting tubulin polymerization. *Biochem J*. 2019;476(10):1401-1417.
- 49 Miyasaka T, Shinzaki Y, Yoshimura S, et al. Imbalanced expression of tau and tubulin induces neuronal dysfunction in C. elegans models of tauopathy. *Front Neurosci*. 2018;12:415.
- 50 Alonso Adel C, Li B, Grundke-Iqbal I, Iqbal K. Polymerization of hyperphosphorylated tau into filaments eliminates its inhibitory activity. *Proc Natl Acad Sci USA*. 2006;103(23):8864-8869.
- 51 Kim KK, Adelstein RS, Kawamoto S. Identification of neuronal nuclei (NeuN) as Fox-3, a new member of the Fox-1 gene family of splicing factors. *J Biol Chem*. 2009;284(45):31052-31061.
- 52 Yamada K, Holth JK, Liao F, et al. Neuronal activity regulates extracellular tau in vivo. *J Exp Med*. 2014;211(3):387-393.
- 53 Alexander GM, Deitch JS, Seeburger JL, Del Valle L, Heiman-Patterson TD. Elevated cortical extracellular fluid glutamate in transgenic mice expressing human mutant (G93A) Cu/Zn superoxide dismutase. *J Neurochem*. 2000;74(4):1666-1673.
- 54 Luo W, Liu W, Hu X, Hanna M, Caravaca A, Paul SM. Microglial internalization and degradation of pathological tau is enhanced by an anti-tau monoclonal antibody. *Sci Rep*. 2015;5:11161.
- 55 Funk KE, Mirbaha H, Jiang H, Holtzman DM, Diamond MI. Distinct therapeutic mechanisms of tau antibodies: promoting microglial clearance versus blocking neuronal uptake. *J Biol Chem*. 2015;290(35):21652-21662.
- 56 Yanamandra K, Jiang H, Mahan TE, et al. Anti-tau antibody reduces insoluble tau and decreases brain atrophy. *Ann Clin Transl Neurol*. 2015;2(3):278-288.
- 57 Kontsekova E, Zilka N, Kovacec B, Skrabana R, Novak M. Identification of structural determinants on tau protein essential for its pathological function: novel therapeutic target for tau immunotherapy in Alzheimer's disease. *Alzheimers Res Ther*. 2014;6(4):45.
- 58 Dekkers G, Bentlage AEH, Stegmann TC, et al. Affinity of human IgG subclasses to mouse Fc gamma receptors. *MAbs*. 2017;9(5):767-773.
- 59 Nimmerjahn F, Ravetch JV. Divergent immunoglobulin g subclass activity through selective Fc receptor binding. *Science*. 2005;310(5753):1510-1512.
- 60 Nimmerjahn F, Bruhns P, Horiuchi K, Ravetch JV. Fc gamma RIV: a novel FcR with distinct IgG subclass specificity. *Immunity*. 2005;23(1):41-51.
- 61 Saylor CA, Dadachova E, Casadevall A. Murine IgG1 and IgG3 isotype switch variants promote phagocytosis of *Cryptococcus neoformans* through different receptors. *J Immunol*. 2010;184(1):336-343.
- 62 Gavin AL, Barnes N, Dijkstra-Hoem HM, Hogarth PM. Identification of the mouse IgG3 receptor: implications for antibody effector function at the interface between innate and adaptive immunity. *J Immunol*. 1998;160(1):20-23.
- 63 Temming AR, Bentlage AEH, de Taeye SW, et al. Cross-reactivity of mouse IgG subclasses to human Fc gamma receptors: Antibody deglycosylation only eliminates IgG2b binding. *Mol Immunol*. 2020;127:79-86.
- 64 Fossati-Jimack L, Ioan-Facsinay A, Reininger L, et al. Markedly different pathogenicity of four immunoglobulin G isotype-switch variants of an antierythrocyte autoantibody is based on their capacity to interact in vivo with the low-affinity Fc gamma receptor III. *J Exp Med*. 2000;191(8):1293-1302.
- 65 Holth JK, Fritsch SK, Wang C, et al. The sleep-wake cycle regulates brain interstitial fluid tau in mice and CSF tau in humans. *Science*. 2019;363(6429):880-884.
- 66 Congdon EE, Gu J, Sait HB, Sigurdsson EM. Antibody uptake into neurons occurs primarily via clathrin-dependent Fc gamma receptor endocytosis and is a prerequisite for acute tau protein clearance. *J Biol Chem*. 2013;288(49):35452-35465.
- 67 Cooper LJ, Shikhman AR, Glass DD, Kangisser D, Cunningham MW, Greenspan NS. Role of heavy chain constant domains in antibody-antigen interaction. Apparent specificity differences among streptococcal IgG antibodies expressing identical variable domains. *J Immunol*. 1993;150(6):2231-2242.
- 68 Pritsch O, Hudry-Clergeon G, Buckle M, et al. Can immunoglobulin C(H)1 constant region domain modulate antigen binding affinity of antibodies? *J Clin Invest*. 1996;98(10):2235-2243.
- 69 Pritsch O, Magnac C, Dumas G, Bouvet JP, Alzari P, Dighiero G. Can isotype switch modulate antigen-binding affinity and influence clonal selection? *Eur J Immunol*. 2000;30(12):3387-3395.
- 70 Hovenden M, Hubbard MA, Aucoin DP, et al. IgG subclass and heavy chain domains contribute to binding and protection by mAbs to the poly gamma-D-glutamic acid capsular antigen of *Bacillus anthracis*. *PLoS Pathog*. 2013;9(4):e1003306.

- 71 Motley MP, Diago-Navarro E, Banerjee K, Inzerillo S, Fries BC. The role of IgG subclass in antibody-mediated protection against carbapenem-resistant *Klebsiella pneumoniae*. *mBio*. 2020;11(5):e02059-20.
- 72 Tudor D, Yu H, Maupetit J, et al. Isotype modulates epitope specificity, affinity, and antiviral activities of anti-HIV-1 human broadly neutralizing 2F5 antibody. *Proc Natl Acad Sci USA*. 2012;109(31):12680–12685.
- 73 Xia Y, Janda A, Eryilmaz E, Casadevall A, Putterman C. The constant region affects antigen binding of antibodies to DNA by altering secondary structure. *Mol Immunol*. 2013;56(1-2):28–37.
- 74 Dam TK, Torres M, Brewer CF, Casadevall A. Isothermal titration calorimetry reveals differential binding thermodynamics of variable region-identical antibodies differing in constant region for a univalent ligand. *J Biol Chem*. 2008;283(46):31366–31370.
- 75 Janda A, Casadevall A. Circular Dichroism reveals evidence of coupling between immunoglobulin constant and variable region secondary structure. *Mol Immunol*. 2010;47(7-8):1421–1425.
- 76 Kato K, Matsunaga C, Odaka A, et al. Carbon-13 NMR study of switch variant anti-dansyl antibodies: antigen binding and domain-domain interactions. *Biochemistry*. 1991;30(26):6604–6610.
- 77 McLean GR, Torres M, Elguezabal N, Nakouzi A, Casadevall A. Isotype can affect the fine specificity of an antibody for a polysaccharide antigen. *J Immunol*. 2002;169(3):1379–1386.
- 78 Torres M, Fernandez-Fuentes N, Fiser A, Casadevall A. The immunoglobulin heavy chain constant region affects kinetic and thermodynamic parameters of antibody variable region interactions with antigen. *J Biol Chem*. 2007;282(18):13917–13927.
- 79 Torres M, Fernandez-Fuentes N, Fiser A, Casadevall A. Exchanging murine and human immunoglobulin constant chains affects the kinetics and thermodynamics of antigen binding and chimeric antibody autoreactivity. *PLoS One*. 2007;2(12):e1310.
- 80 Torres M, May R, Scharff MD, Casadevall A. Variable-region-identical antibodies differing in isotype demonstrate differences in fine specificity and idiotype. *J Immunol*. 2005;174(4):2132–2142.
- 81 Xia Y, Pawar RD, Nakouzi AS, et al. The constant region contributes to the antigenic specificity and renal pathogenicity of murine anti-DNA antibodies. *J Autoimmun*. 2012;39(4):398–411.
- 82 Yuan RR, Spira G, Oh J, Paizi M, Casadevall A, Scharff MD. Isotype switching increases efficacy of antibody protection against *Cryptococcus neoformans* infection in mice. *Infect Immun*. 1998;66(3):1057–1062.